About Omics Group

OMICS Group International through its Open Access Initiative is committed to make genuine and reliable contributions to the scientific community. OMICS Group hosts over 400 leading-edge peer reviewed Open Access Journals and organize over 300 International Conferences annually all over the world. OMICS Publishing Group journals have over 3 million readers and the fame and success of the same can be attributed to the strong editorial board which contains over 30000 eminent personalities that ensure a rapid, quality and quick review process.

About Omics Group conferences

- OMICS Group signed an agreement with more than 1000 International Societies to make healthcare information Open Access. OMICS Group Conferences make the perfect platform for global networking as it brings together renowned speakers and scientists across the globe to a most exciting and memorable scientific event filled with much enlightening interactive sessions, world class exhibitions and poster presentations
- Omics group has organised 500 conferences, workshops and national symposium across the major cities including SanFrancisco,Omaha,Orlado,Rayleigh,SantaClara,Chicago ,Philadelphia,Unitedkingdom,Baltimore,SanAntanio,Dubai ,Hyderabad,Bangaluru and Mumbai.

Nano Engineering
Research Group

AIR FORCE OFFICE OF SCIENTIFIC RESEARCH
UNITED STATES AIR FORCE

University Of Illinois
at Chicago
College Of Engineering

Design of a Novel Heterostructure Photodetectors with Dramatically Enhanced Signal-to-Noise based on Resonant Interface-Phonon-Assisted Transitions and Engineering of Energy States to Enhance Transition Rates

Yi Lan[a], Nanzhu Zhang[a], Lucy Shi[a], Chenjie Tang[a], Mitra Dutta[a,b], and Michael A. Stroscio[a,b,c]

Optics-2014, 8-10 Sept. 2014

[a]Electrical and Computer Engineering Department, U. of Illinois at Chicago (UIC), 851 S. Morgan Street, Chicago, Illinois 60607
[b]Physics Department, U. of Illinois at Chicago, 851 S. Morgan Street, Chicago, Illinois
[c]Bioengineering Department, U. of Illinois at Chicago, 851 S. Morgan St., Chicago, IL

Nano Engineering
Research Group

AIR FORCE OFFICE OF SCIENTIFIC RESEARCH
UNITED STATES AIR FORCE

University Of Illinois
at Chicago
College Of Engineering

A novel heterostructure photodetector design is presented that facilitates dramatic enhancements of signal-to-noise. The structure incorporates a single quantum well coupled to a symmetric double quantum well that makes it possible to engineer energy states with energy state separations equal to an interface phonon energy. In addition, quantum level energy degeneracy between states in the single-well and double-well systems makes it possible to enhance the rate of interface-phonon-assisted transitions. The techniques underlying this approach have been discussed previously by Stroscio and Dutta in Phonons in Nanostructures (Cambridge University Press, 2001). Together, these effects make it possible to greatly enhance signal-to-noise ratios in these heterostructure-based photodetectors. These designs are optimized based on Schrödinger equation calculations of the energy states and the determination of interface phonon potentials and dispersion modes by applying boundary conditions for which the phonon potential has corresponding continuous normal components of the displacement field and tangential components of electric fields. Novel photodetector designs with dramatically enhanced signal-to-noise will be presented for a number of different heterostructure devices.

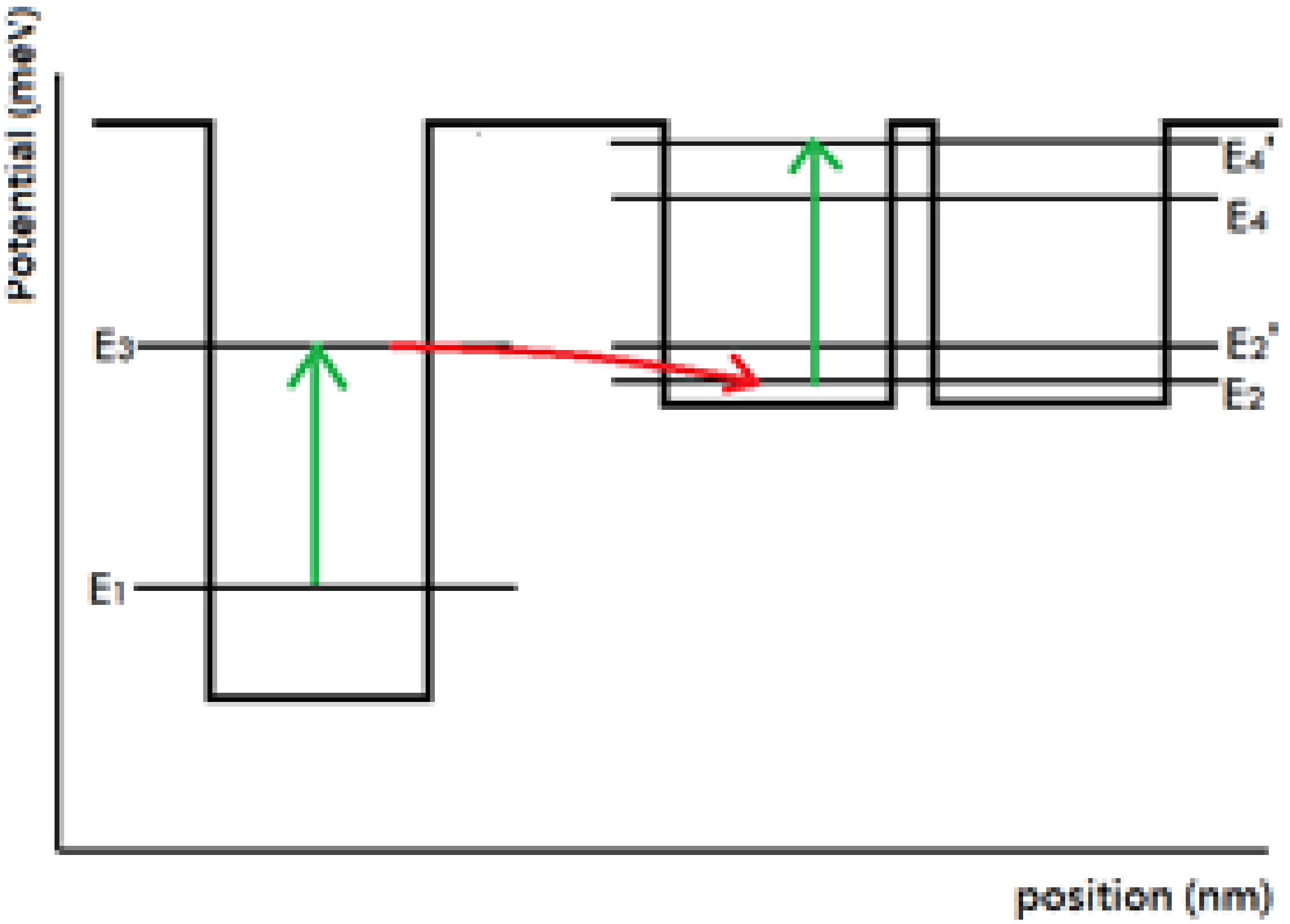
Potential (meV)
E4'
E4
E3
E2'
E2
E1
position (nm)

This energy-level structure facilitates the absorption of a photon, emission of a phonon, and the absorption of a photon with the same wavelength as the original photon. E_1 is the first energy level of the single well, and E_3 is the second energy level. In addition, E_2, $E_{2'}$, E_4, and $E_{4'}$ represent the first, second, third, and forth energy levels for the double quantum well.

With reference to Fig. 1, it is straightforward to see that there will be a dramatic signal-to-noise enhancement in the current, $I_{sn,E1}$, from the deepest state E_1, relative to $I_{sn,E2}$, from the deepest state E_2 (without phonon-assisted transition and second photon absorption), as given by the Richardson formula:

$$\frac{I_{sn,E_1}}{I_{sn,E_2}} = \frac{e^{-\frac{2E_{photon}-E_{phonon}}{kT}}}{e^{-\frac{E_{photon}}{kT}}} = e^{-\frac{E_{photon}-E_{phonon}}{kT}}$$

In this equation, $E_3 - E_1 = E_{4'} - E_2 =$ Ephoton and $E_{2'} - E_2 = E_{phonon}$.

For example if,

$$\frac{E_{photon}-E_{phonon}}{kT} = 8$$

a dramatic 1/3,000 reduction can be realized.

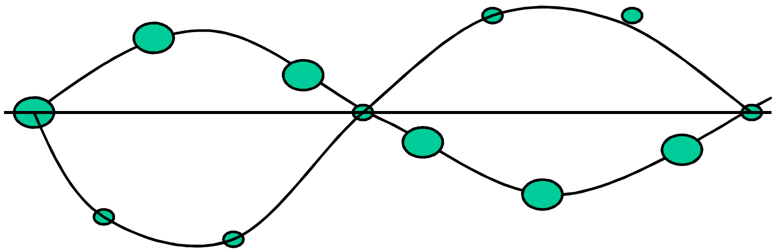

Transverse Optical (TO) Phonon

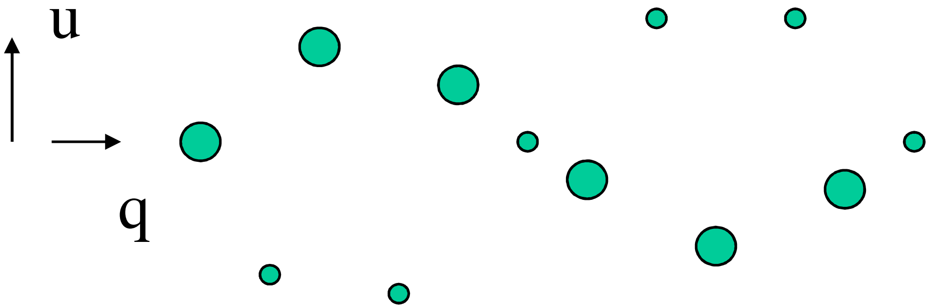

Transverse Optical (TO) Phonon
u – displacement
q - direction

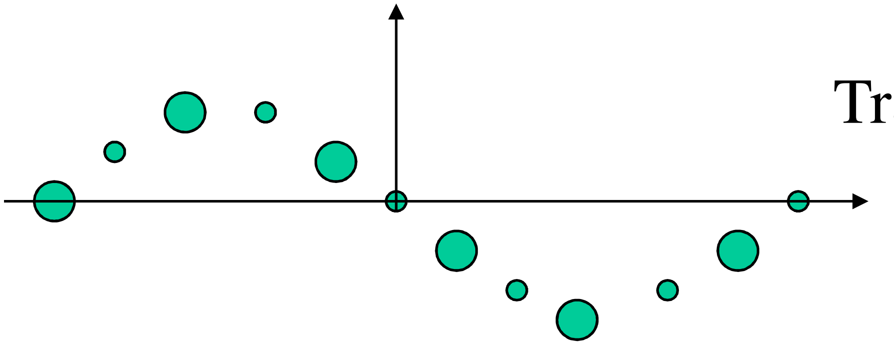

Transverse Acoustic (TA) Phonon

LO and LA Phonons have displacements along the direction of q

Phonons: Some Basic Characteristics

Boundary Conditions:

Optical modes --- continuity of the tangential component of the electric field and the z component of the displacement vector must be continuous at the interfaces

Acoustic modes --- displacement and normal component of stress tensor are continuous at interfaces

For example $$\varepsilon_{j,z}\left.\frac{\partial \phi_j(z)}{\partial z}\right|_{z=z_j} = \varepsilon_{j+1,z}\left.\frac{\partial \phi_{j+1}(z)}{\partial z}\right|_{z=z_j}$$

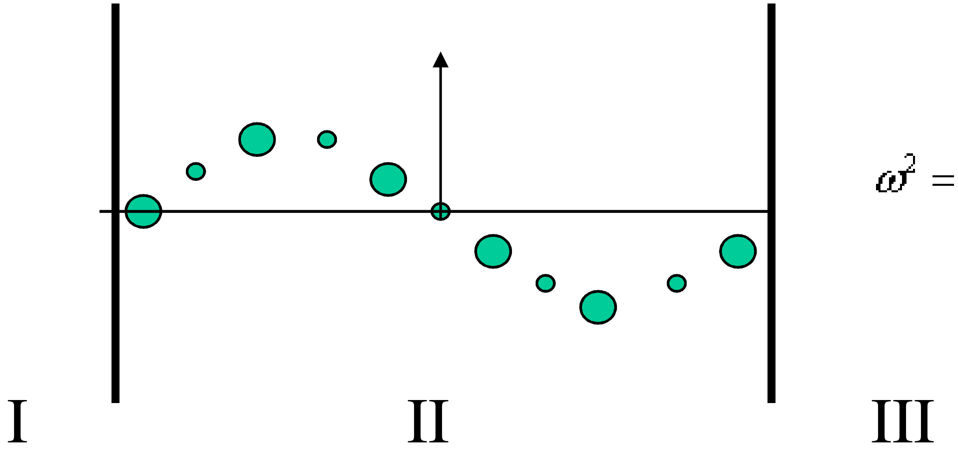

$$\omega^2 = C\left(\frac{1}{M_1}+\frac{1}{M_2}\right) \pm C\sqrt{\left(\frac{1}{M_1}+\frac{1}{M_2}\right)^2 - \frac{4\sin^2\left(\frac{ka}{2}\right)}{M_1 M_2}}$$

↓

Quantized Confined Phonons

Normalization and Applicability of Elastic Continuum Theory --- One Monolayer Thick?

Normalization:

Mode amplitude normalized so that the energy in each model is the quantized phonon energy – example 2D graphene

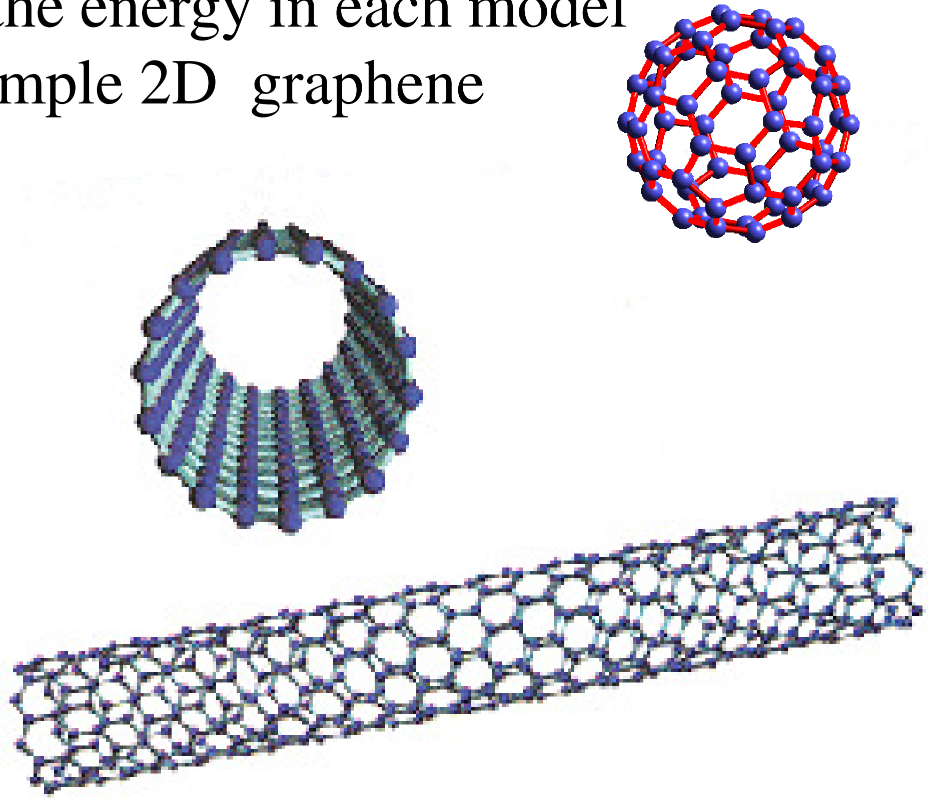

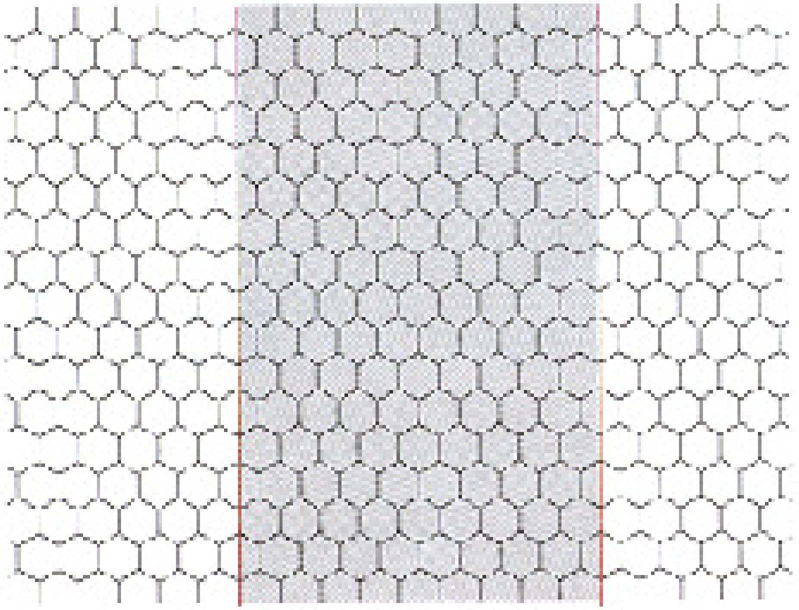

$$\frac{1}{S}\int_{s}\left(u\cdot u^{*}+v\cdot v^{*}\right)dxdy=\frac{\hbar}{2M\,\omega_{mn}^{LO}}$$

Elastic Continuum Theory Gives Correct Energy for a Dominant Mode of the Nanomechanical Modes in Carbon Nanotubes and in C_{60}

McEwen & Park et al., Nature
September 2000

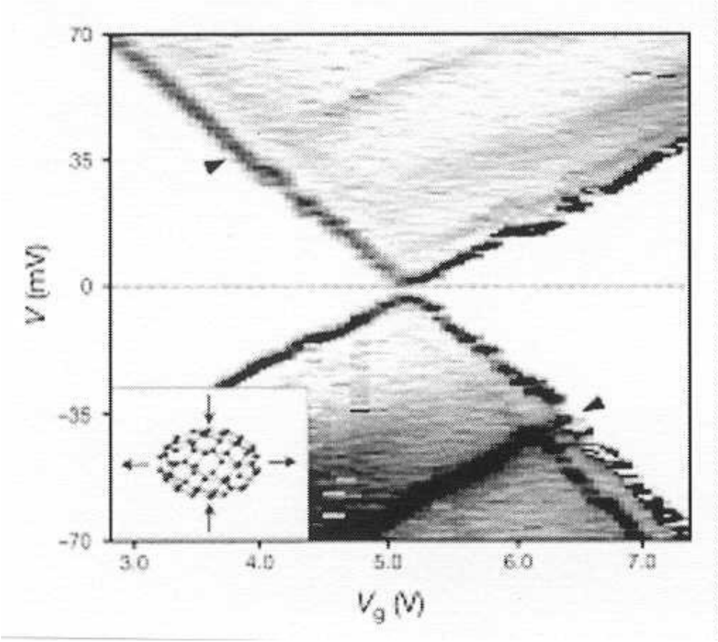

35 meV mode observed experimentally

Elastic Continuum Results

Mode Energy (meV)

a_0	62
a_1	74
a_2	111
b_2	32
b_3	38

Matches our theoretical results to 10%

Goal: Theoretical Description of Nanoscale Mechanical Structures for Nanodevice and Sensor Applications including Nanocantilevers

Phonons: Some Basic Characteristics

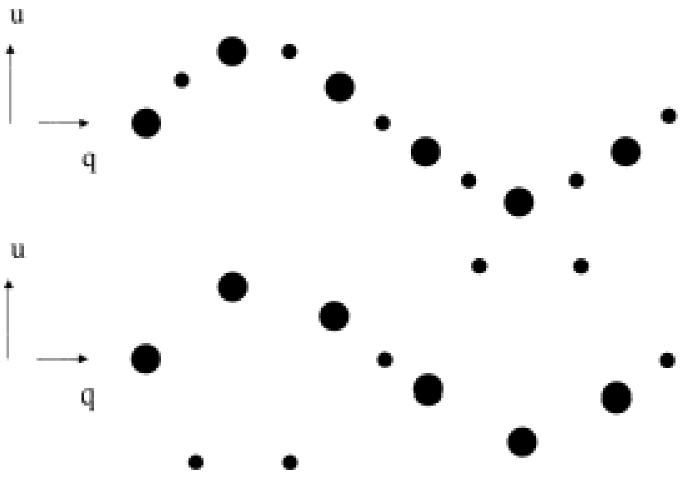

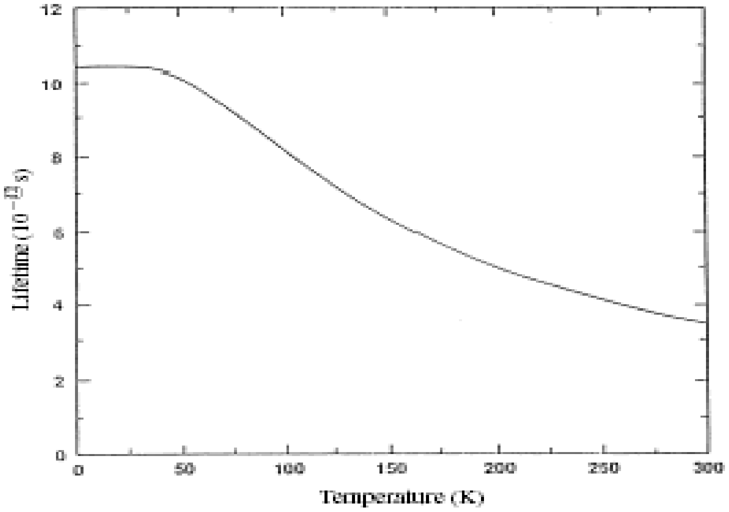

Figure 6.2. LO phonon lifetime in GaAs as a function of temperature. From Bhatt et al. (1994), American Institute of Physics, with permission.

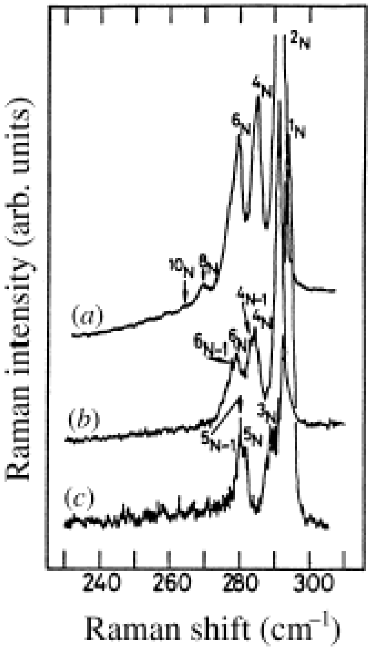

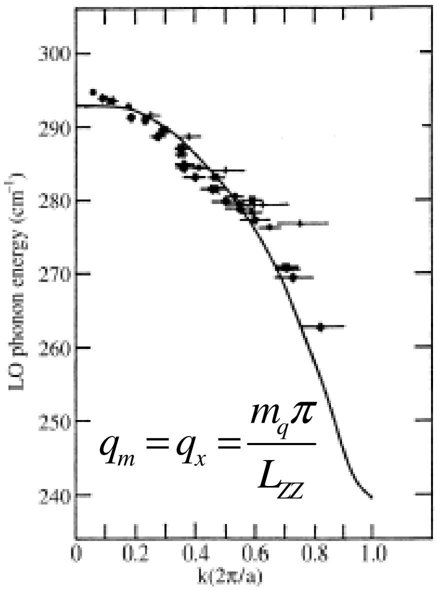

$$q_m = q_x = \frac{m_q \pi}{L_{ZZ}}$$

Precision and Nature of
Optical Phonon Confinement
H. Sakaki et al.

Anharmonic Effects:
Klemen’s Channel with Keating Model ---Bhatt, Kim and Stroscio

Selection of Major Theoretical Papers: Optical Modes

- **R. Fuchs and K. L. Kliewer**, **"Optical Modes of Vibration in an Ionic Slab,"** Physical Review, 140, A2076-A2088 (1965).
- **J. J. Licari and R. Evrard**, **"Electron-Phonon Interaction in a Dielectric Slab: Effect of Electronic Polarizability,"** Physical Review, B15, 2254-2264 (1977).
- **L. Wendler**, **"Electron-Phonon Interaction in Dielectric Bilayer System: Effects of Electronic Polarizability,"** Physics Status Solidi B, 129, 513-530 (1985).
- **C. Trallero-Giner, F. Garcia-Moliner, V. R. Velasco, and M. Cardona**, **"Analysis of the Phenomenological Models for Long-Wavelength Polar Optical Modes in Semiconductor Layered Systems,"** Physical Review, B45, 11,944-11,948 (1992).
- **K. J. Nash**, **"Electron-Phonon Interactions and Lattice Dynamics of Optic Phonons in Semiconductor Heterostructures,"** Physical Review, B46, 7723-7744 (1992). --- For slab modes, reformulated slab vibrations, and guided modes, "intrasubband and intersubband electron-phonon scattering rates are **independent of the basis set used to describe the modes, as lond as this set is orthogonal and complete**."
- **F. Comas, C. Trallero-Giner, and M. Cardona**, **"Continuum Treatment of Phonon Polaritons in Semiconductor Heterostructures,"** Physical Review, B56, 4115-4127 (1997). --- Seven coupled partial differential equations; solutions for isotropic materials; **the non-dispersive case "leads to the the Fuchs-Kliewer slab modes."**

More on Confined, Interface, and Half-Space Phonon Modes

in

Phonons and Nanostructures

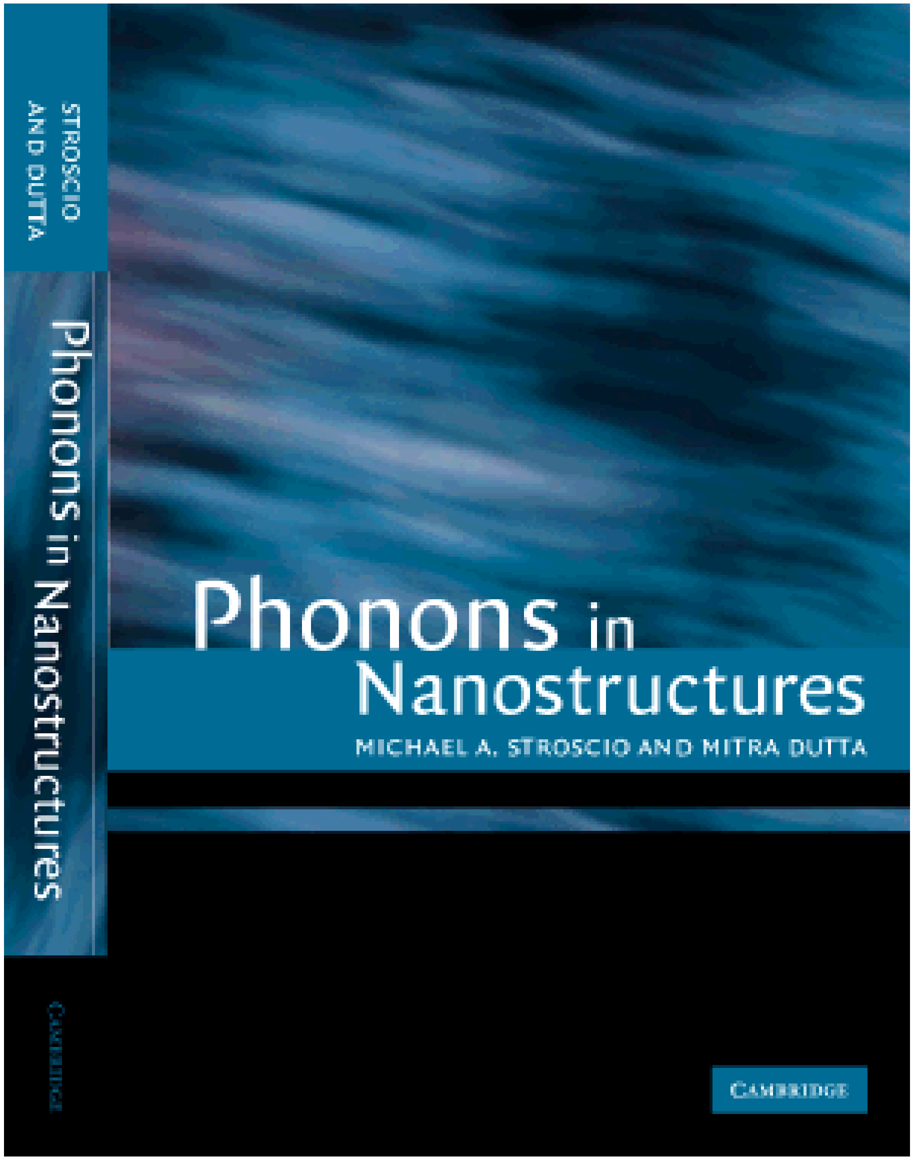

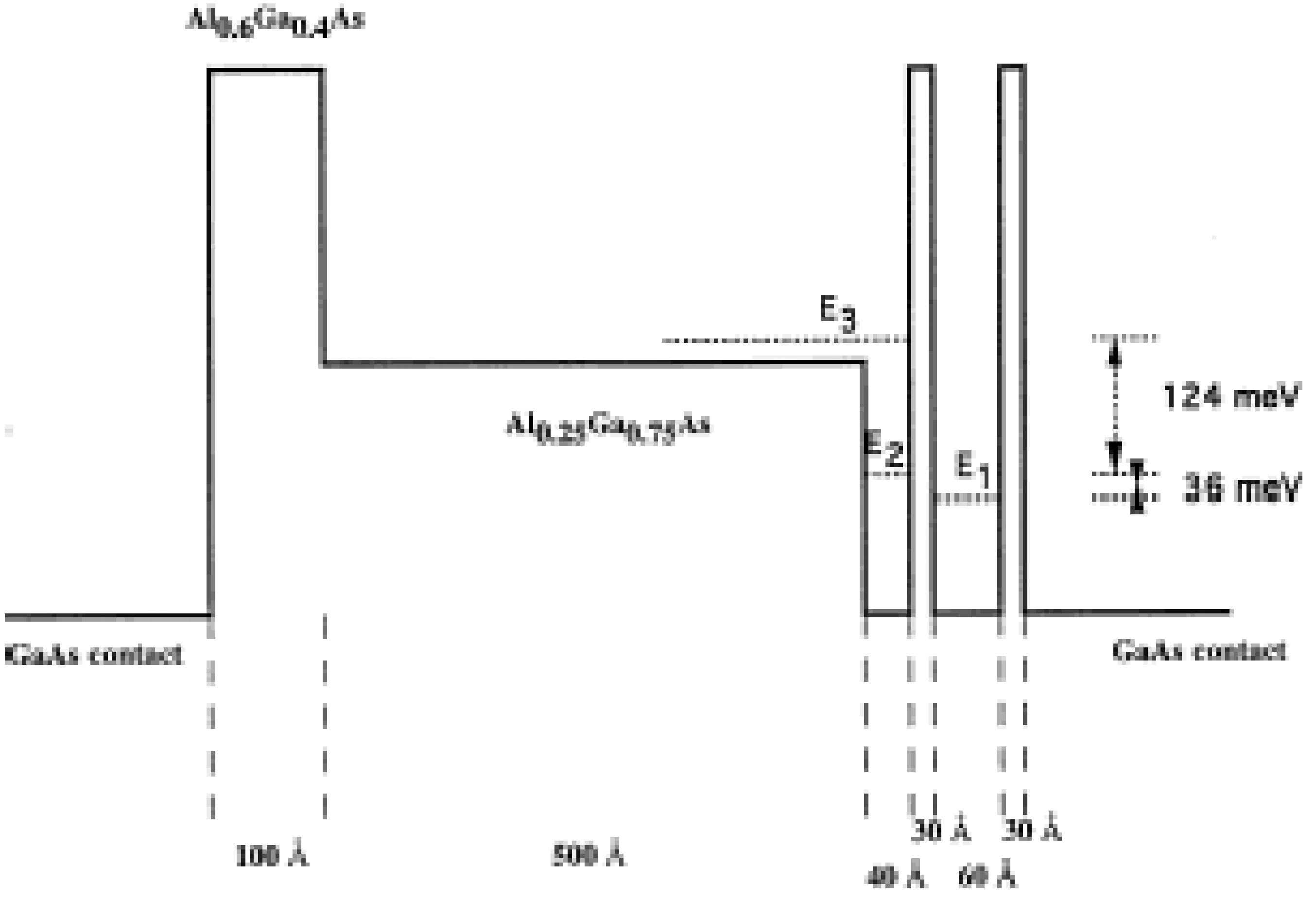
$Al_{0.6}Ga_{0.4}As$
E$_3$
124 meV
$Al_{0.25}Ga_{0.75}As$
E$_2$
E$_1$
36 meV
GaAs contact
GaAs contact
30 Å
30 Å
100 Å
500 Å
40 Å
60 Å

More on Interface Modes

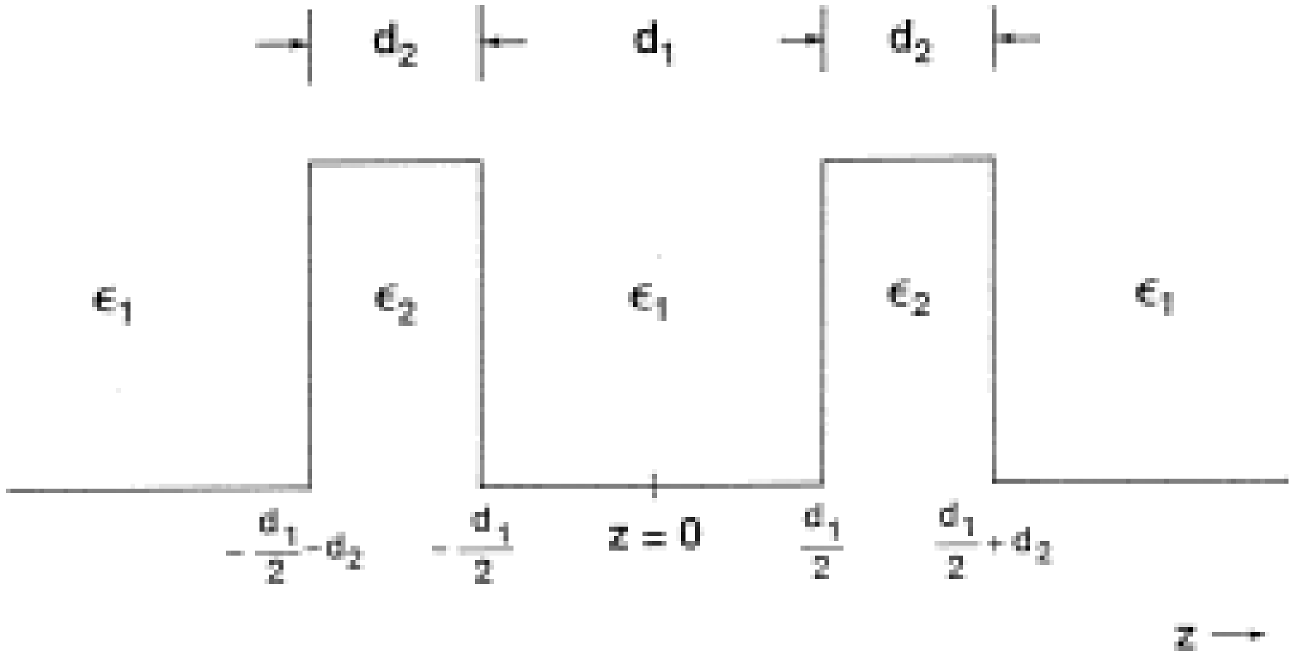

More on Interface Modes

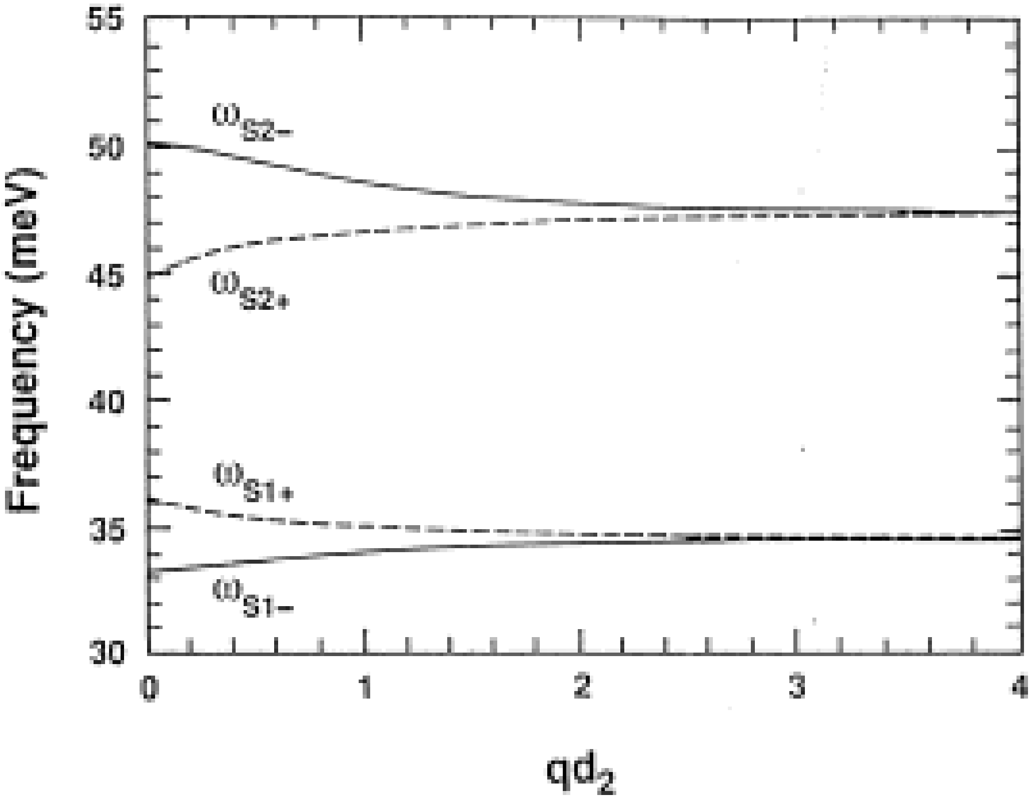

More on Interface Modes

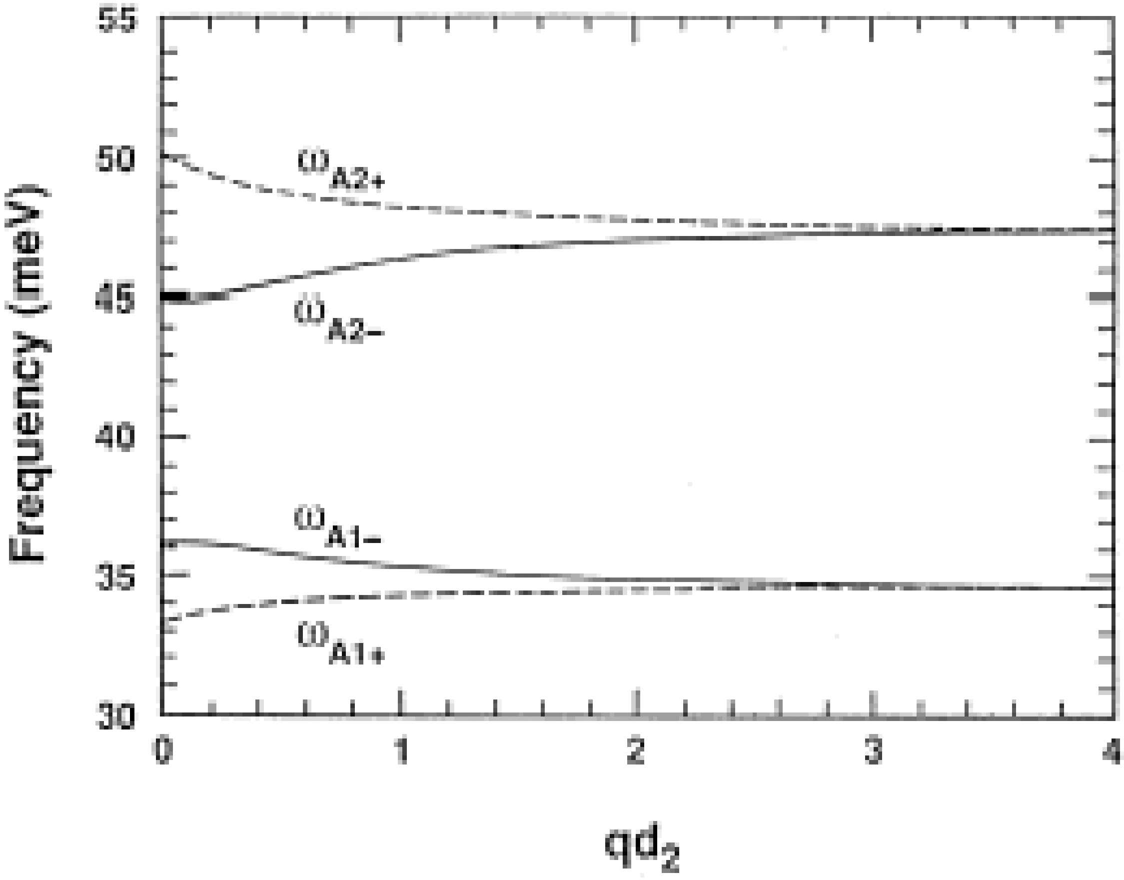

More on Interface Modes

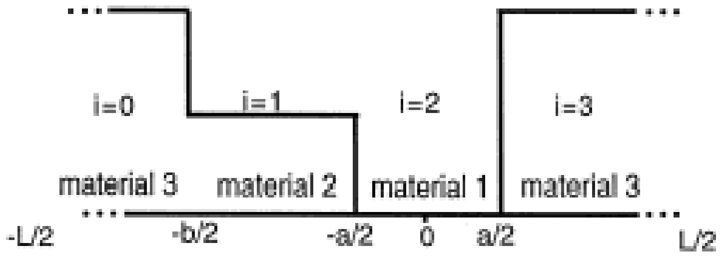

(a)

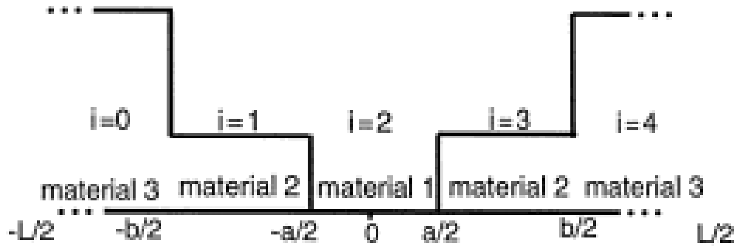

(b)

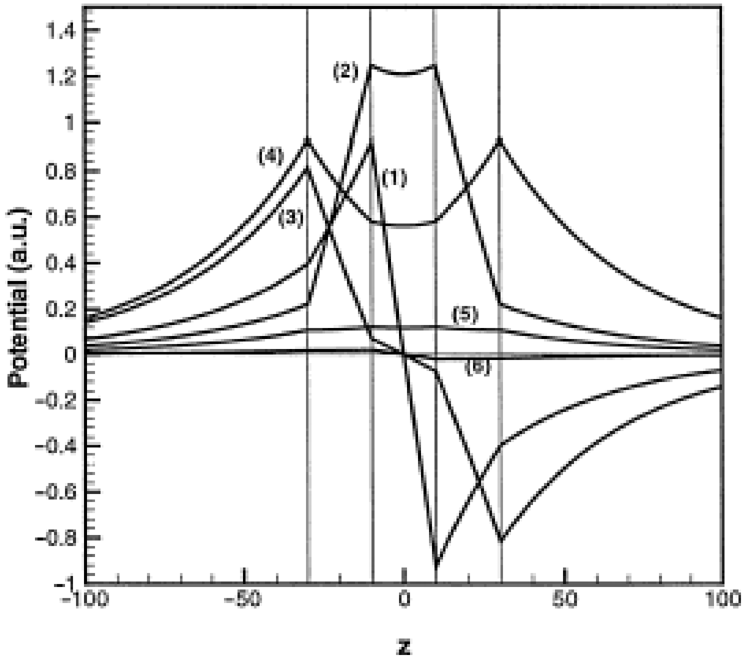

Phonon “Bands”

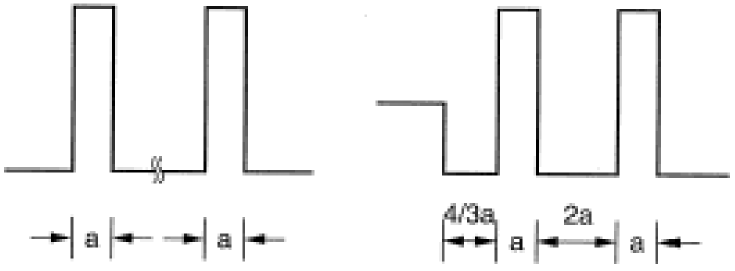

(*a*) (*b*)

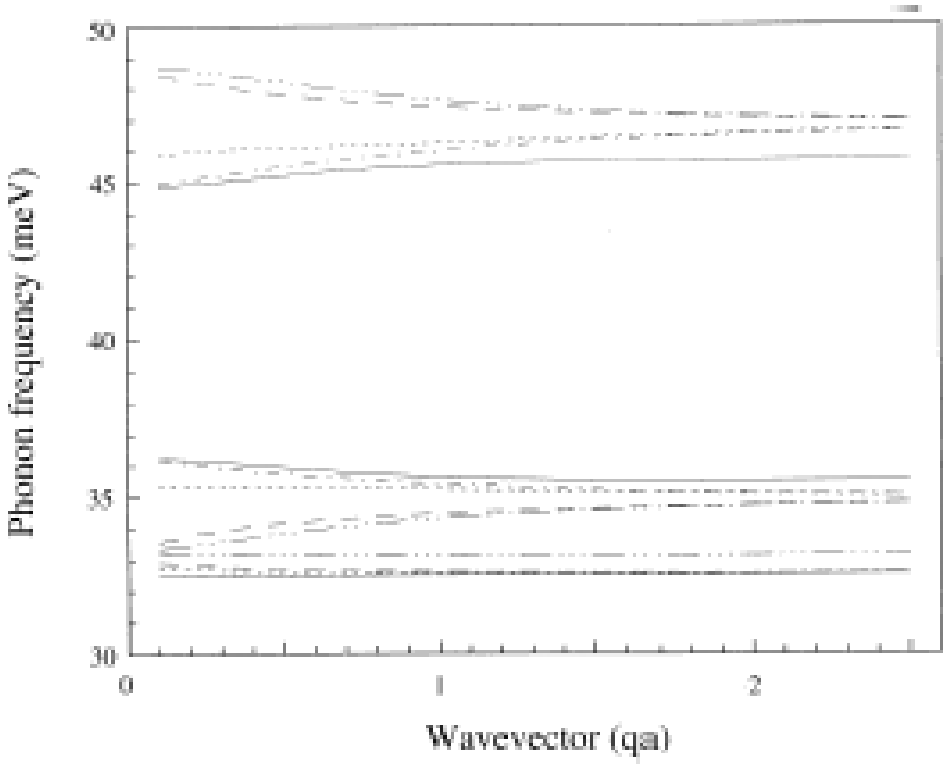

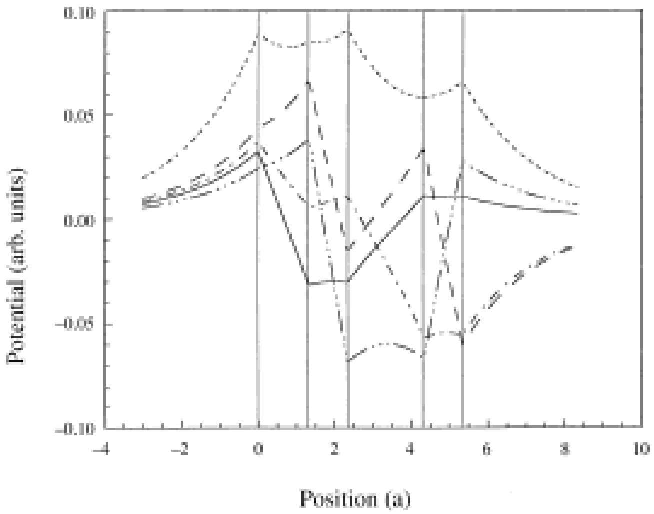

Phonon "Bands"

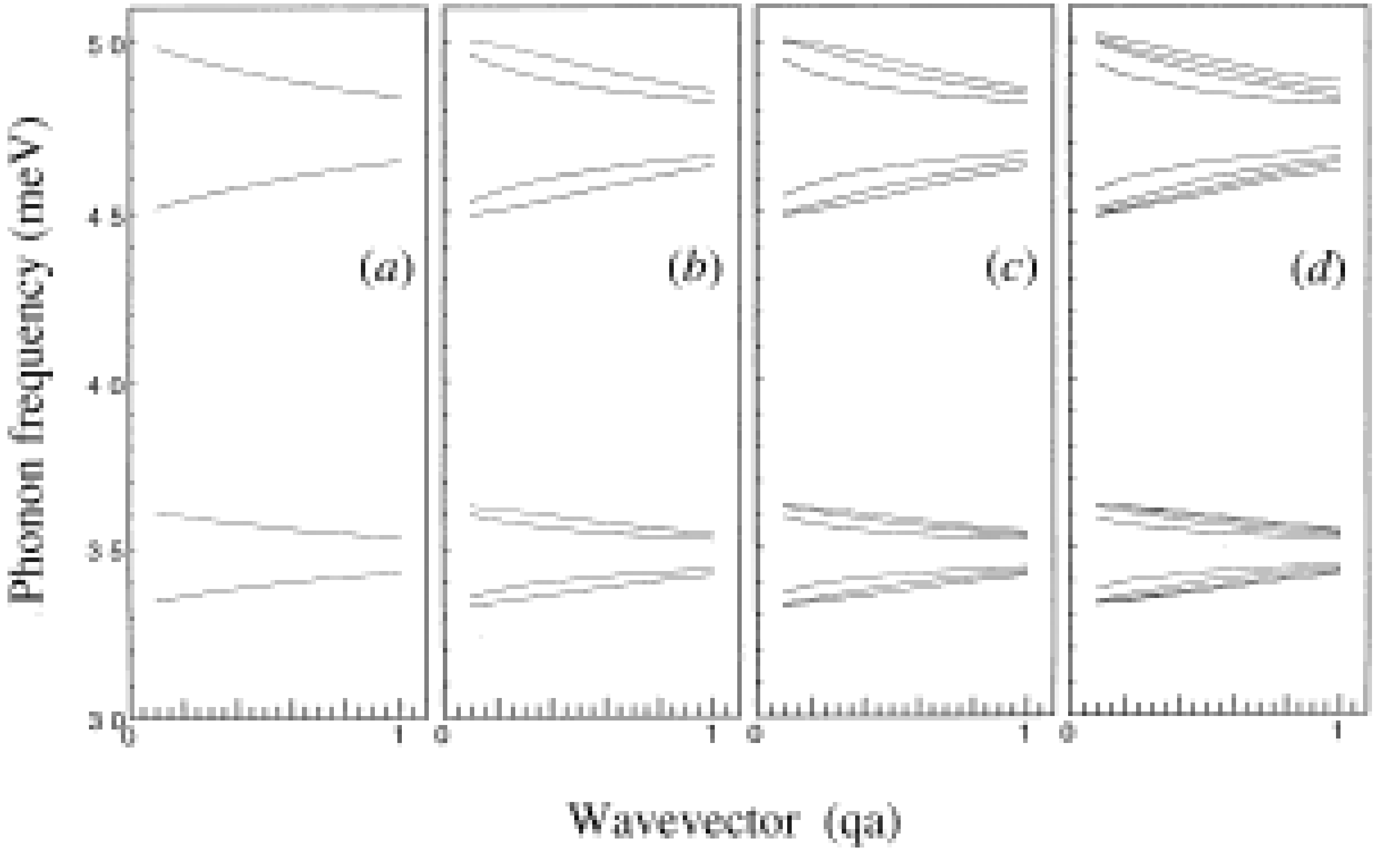

Improved Semiconductor Lasers via Phonon-Assisted Transitions

Key Point -- Optical Devices not Electronic Devices!

Why? <u>ENERGY SELECTIVITY</u>

<u>A single engineered phonon mode may be selected to modify a selected interaction</u>

Interface Optical Phonons: Applications to Phonon-Assisted Transitions in Heterojunction Lasers

---

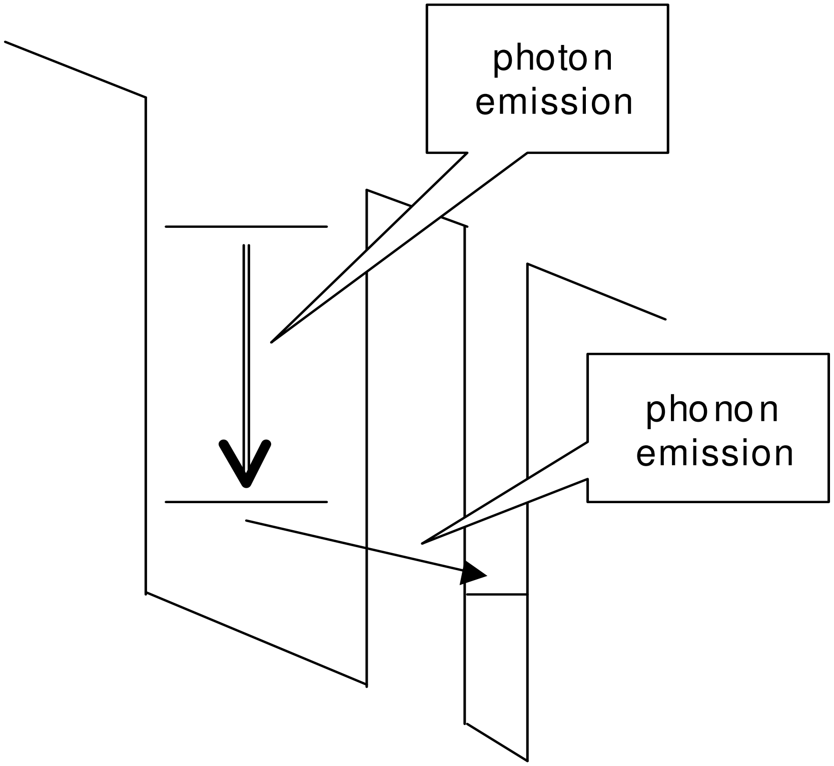

Interface-Phonon-Assisted Processes: Double Resonance Process

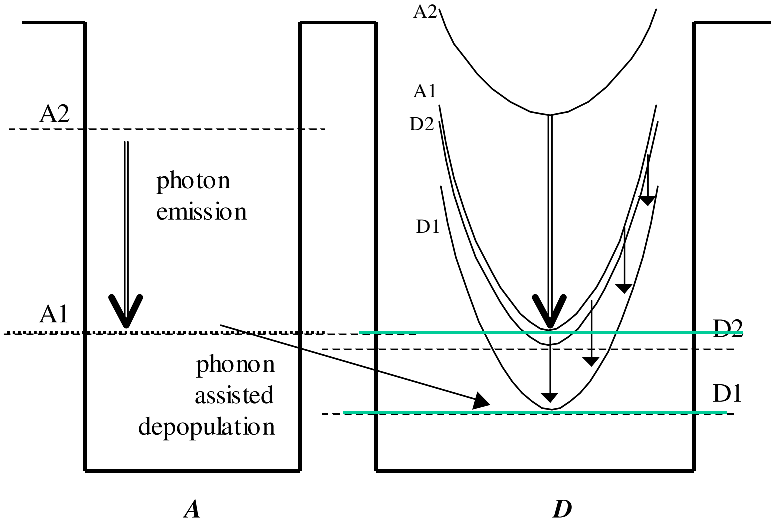

Gain enhancements greater than two orders of magnitude

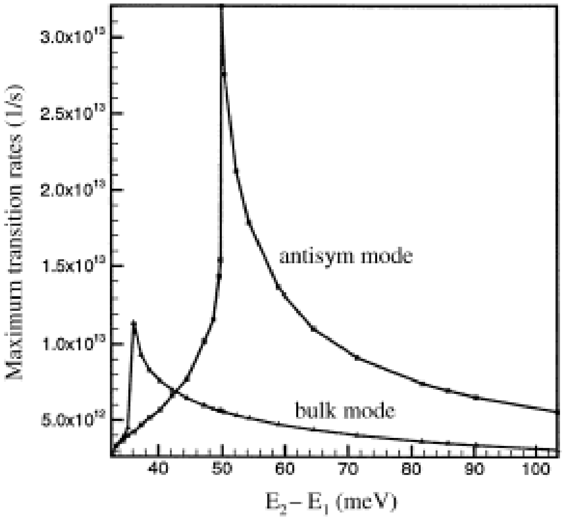

Interface phonon modes dominate over bulk modes

APPLIED PHYSICS LETTERS VOLUME 75, NUMBER 21 22 NOVEMBER 1999

Phonon enhanced inverse population in asymmetric double quantum wells

Michael A. Stroscio
U.S. Army Research Office, P.O. Box 12211, Research Triangle Park, North Carolina 27709-2211

Mikhail Kisin,[a] Gregory Belenky, and Serge Luryi
Department of Electrical and Computer Engineering, State University of New York at Stony Brook, New York 11794-2350

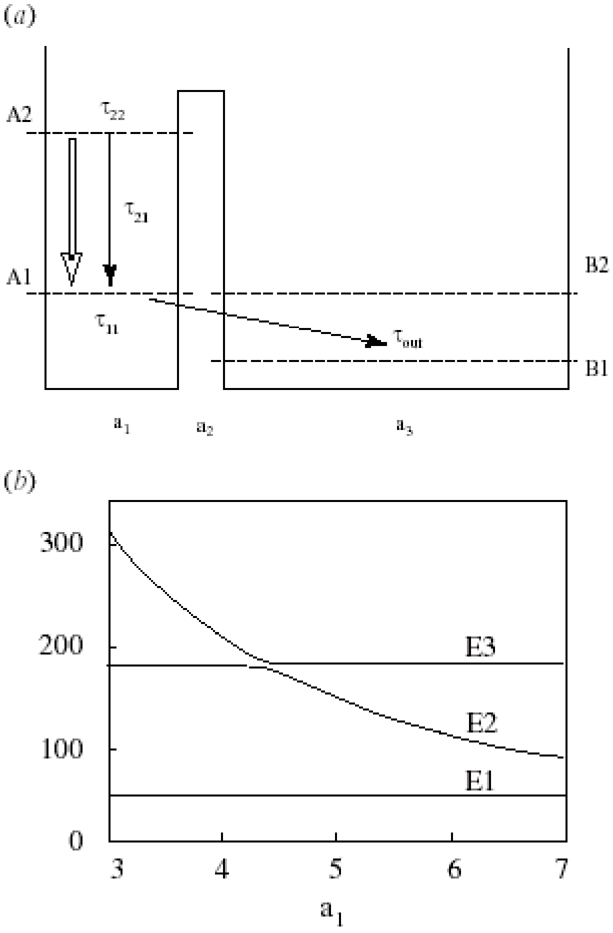

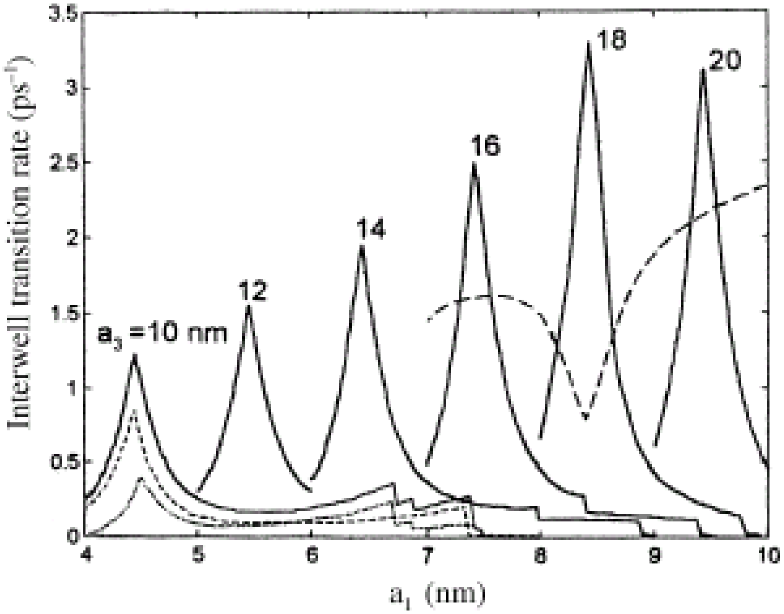

a_2 = 2 nm, a_3 = 10 nm

$$\eta_{tot} = n_{A2} / n_{A1} = \tau_{21}/\tau_{out}$$
$$= 6 \text{ for } a_1 = 8.5 \text{ nm}$$
$$\eta_{loc} = (n_{A2} / n_{A1})_{k=0}$$
$$= \eta_{tot} (1 + \tau_{11}/ \tau_{out})^{EA2\text{-}A1/Ephonon}$$
$$\geq 50 - 100$$

APPLIED PHYSICS LETTERS VOLUME 75, NUMBER 21 22 NOVEMBER 1999

Phonon enhanced inverse population in asymmetric double quantum wells

Michael A. Stroscio
U.S. Army Research Office, P.O. Box 12211, Research Triangle Park, North Carolina 27709-2211

Mikhail Kisin,[a)] Gregory Belenky, and Serge Luryi
Department of Electrical and Computer Engineering, State University of New York at Stony Brook, New York 11794-2350

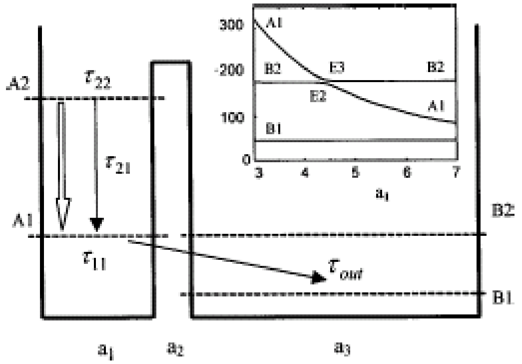

FIG. 1. Model band diagram and energy levels of an AlAs/GaAs double quantum well heterostructure. Double-lined arrow corresponds to the light-emitting transition in the heterostructure. The inset shows the positions of three lowest subbands (in meV) as a function of the narrow well width a_1 (in nm) for fixed values $a_2 = 2$ nm and $a_3 = 10$ nm.

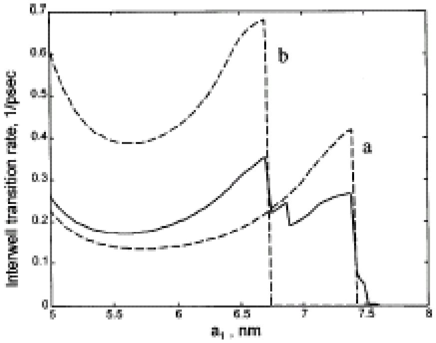

FIG. 2. Onset for the interwell electron-phonon resonance. Solid line shows the total $A1-B1$ transition rate by all confined and interface LO-phonon modes of a double quantum well heterostructure as a function of the narrow well width a_1. Here $a_2 = 2$ nm and $a_3 = 10$ nm. Two dashed curves represent the interwell transition rates calculated in the single-mode bulk-like LO-phonon spectrum approximation with phonon energies: (a) $\hbar\omega_{LO}^{GaAs} = 36$ meV, and (b) $\hbar\omega_{LO}^{AlAs} = 51$ meV.

transitions indirect in real space.[11] The exemplary intrawell $A2-A1$ phonon-emission rate for the heterostructure with $a_3 = 18$ nm is shown in Fig. 3 by the bold dashed line. The total intersubband population ratio, η_{tot}, can be roughly estimated as $\eta_{tot} = n_{A2}/n_{A1} \approx \tau_{21}/\tau_{out}$ and under the double resonance condition ($a_1 = 8.5$ nm) it is as high as $\eta_{tot} \approx 6$, whereas outside the resonance region the total population inversion disappears. Thus for $a_1 = 8.0$ nm, we have only $\eta_{tot} \approx 0.5$. It is worth noting that the total subband populations determine the optical gain and the output power only in the high electron concentration limit.[12] For low electron concentrations $n_A \leq 10^{11}$ cm^{-2}, the lasing action is governed by the local nonequilibrium k-space population inversion between $A2$ and $A1$ subband bottoms which cannot be reduced to η_{tot}. In this case, the interwell depopulation rate becomes

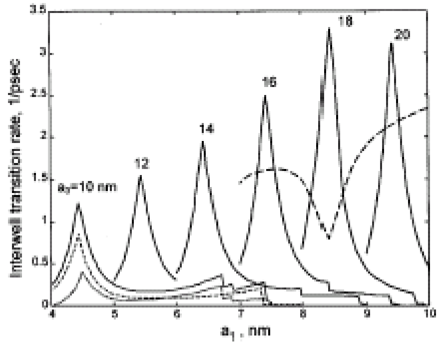

FIG. 3. Peak values of the interwell optical-phonon-assisted transition rate under the double electron-phonon resonance condition. The curves are labeled with the value of the wider quantum well width a_3 in nm. Curve 10 details individual contributions to the overall phonon-emission rate: dashed line-confined phonon modes, dotted line-interface phonon modes. Bold dashed line represents the rate of the nonradiative intrawell intersubband transitions, τ_{21}^{-1}, for the heterostructure with $a_3 = 18$ nm.

even more important. Assuming that $A2$ electrons are distributed in a narrow region near the subband bottom we have[3,12]

$$\eta_{loc} = \left(\frac{n_{A2}}{n_{A1}}\right)_{k=0} \approx \eta_{tot}\left(1 + \frac{\tau_{11}}{\tau_{out}}\right)^{E_{A2A1}/\hbar\omega_{ph}}.$$

For a large $A2-A1$ separation and low values of τ_{out} the local population inversion can be significantly enhanced. For the double-quantum-well heterostructure with $a_1 = 8.5$ nm, $a_2 = 2$ nm, and $a_3 = 18$ nm, we find $\tau_{11}/\tau_{out} \approx 0.6$ and $E_{A2A1}/\hbar\omega_{LO}^{GaAs} \approx 5$, which results in $\eta_{loc} \approx 10\eta_{tot}$ and may be very favorable for the overall laser performance.

It should be clearly understood, however, that population inversion is not the only important parameter for a successful laser design. For instance, care must be taken to minimize the leakage of electrons from the upper lasing level $A2$ through a third energy level $B3$ of the wide well, which shunts the useful injection current. This process has little effect on the population inversion but it increases the lasing threshold. For our exemplary heterostructure, calculations show that the level $B3$ can be located within less than one $\hbar\omega_{ph}$ from the level $A2$, thus suppressing phonon-assisted leakage, by taking the active quantum well width $a_1 \approx 11.5$ nm and applying an external electric field 8 kV/cm to satisfy the double electron-phonon resonance condition.

Interface-Phonon-Assisted Processes

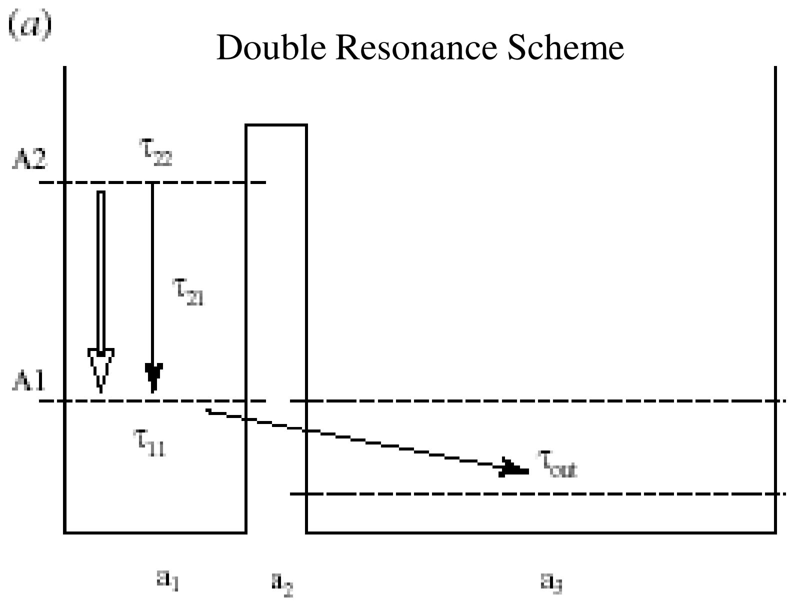

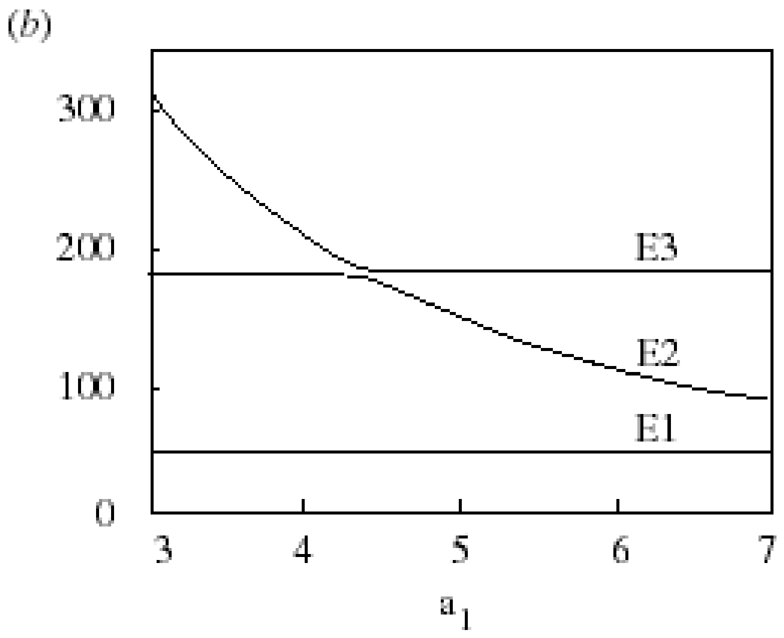

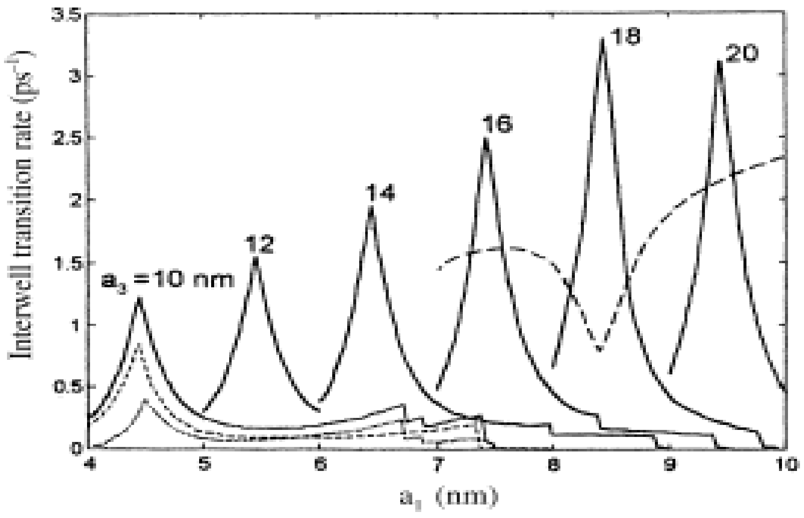

ps transition rates

Michael A. Stroscio, Mikhail V. Kisin, Gregory Belenky, and Serge Luryi, Phonon Enhanced Inverse Population in Asymmetric Double Quantum Wells, Applied Physics Letters, 75, 3258 (1999).

Interface-Phonon-Assisted Processes

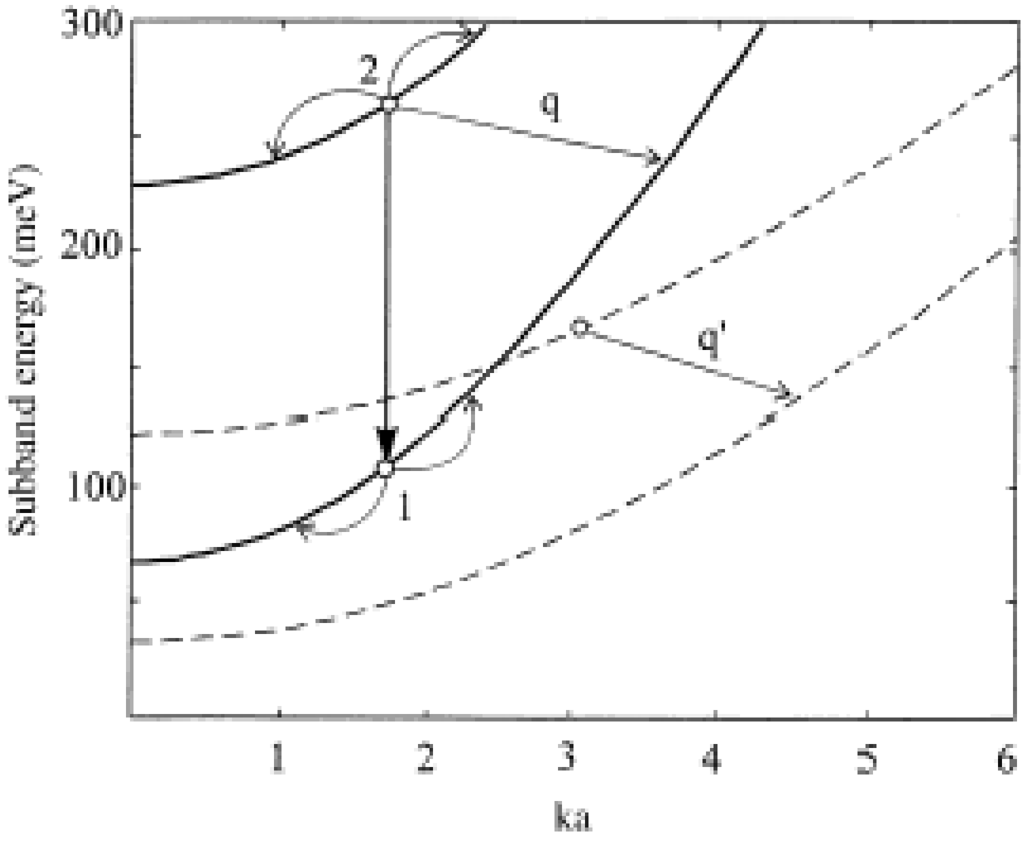

Figure 10.7. Energy dispersion curves for 60-ångstrom-wide (solid lines) and 100-ångstrom-wide (broken lines) $Al_{0.3}Ga_{0.7}As/GaAs/Al_{0.3}Ga_{0.7}As$ quantum wells. Typical intersubband and intrasubband transitions are shown for both quantum wells. The energy gap for the GaAs well, E_g(GaAs), is taken as 1.4 eV and the ratio of the effective mass to the electron mass is taken as 0.067 for GaAs. From Kisin *et al.* (1997), American Institute of Physics, with permission.

References 4 and 5:

M. Kisin, M. Stroscio, V. Gorfinkel, G. Belenky and S. Luryi, Influence of Complex Phonon Spectrum of Heterostructure on Gain Lineshape in Quantun Cascade Laser (QCL), Optical Society of America, Technical Digest Series, Volume 11, 425 (1997).

Mikhail V. Kisin, Vera B. Gorfinkel, Michael A. Stroscio, Gregory Belenky, and Serge Luryi, Influence of Complex Phonon Spectra on Intersubband Optical Gain, J. Appl. Phys., 82, 2031 (1997).

----- 10 nm
____ 6 nm

AlGaAs-GaAs-AlGaAs
x = 0.3

Interface-Phonon-Assisted Processes, Con't

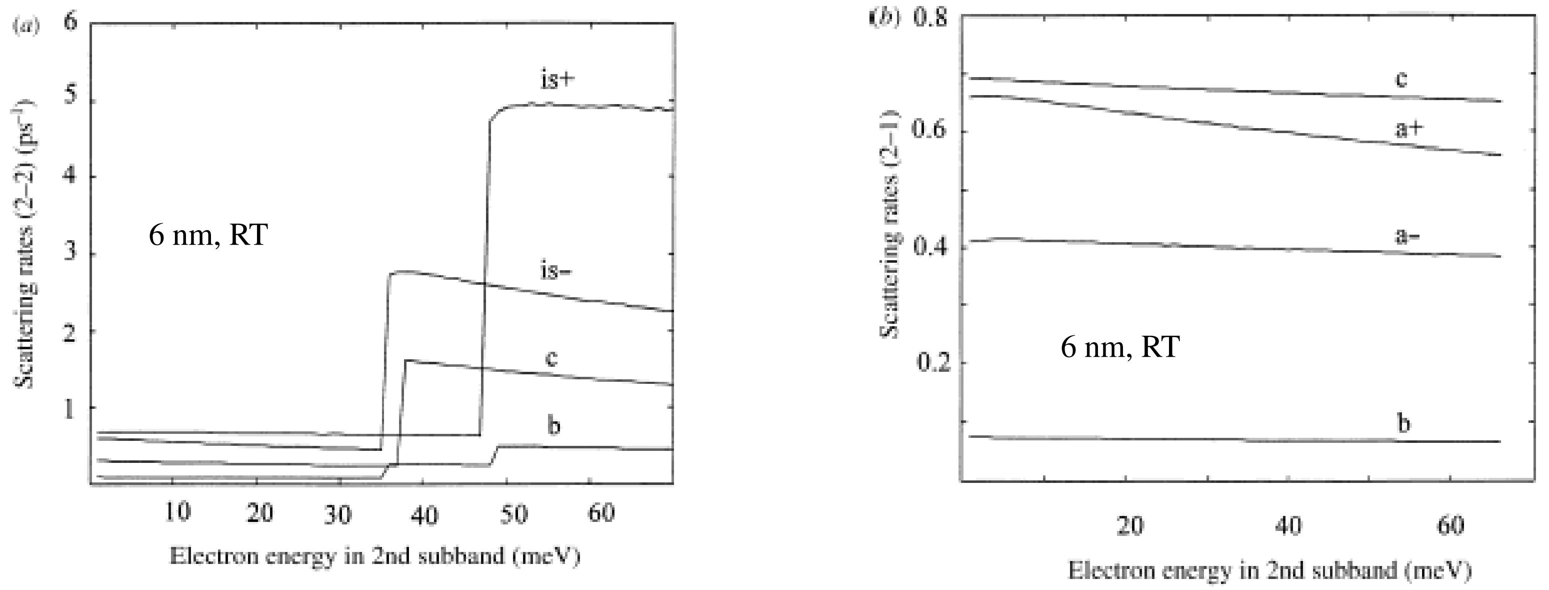

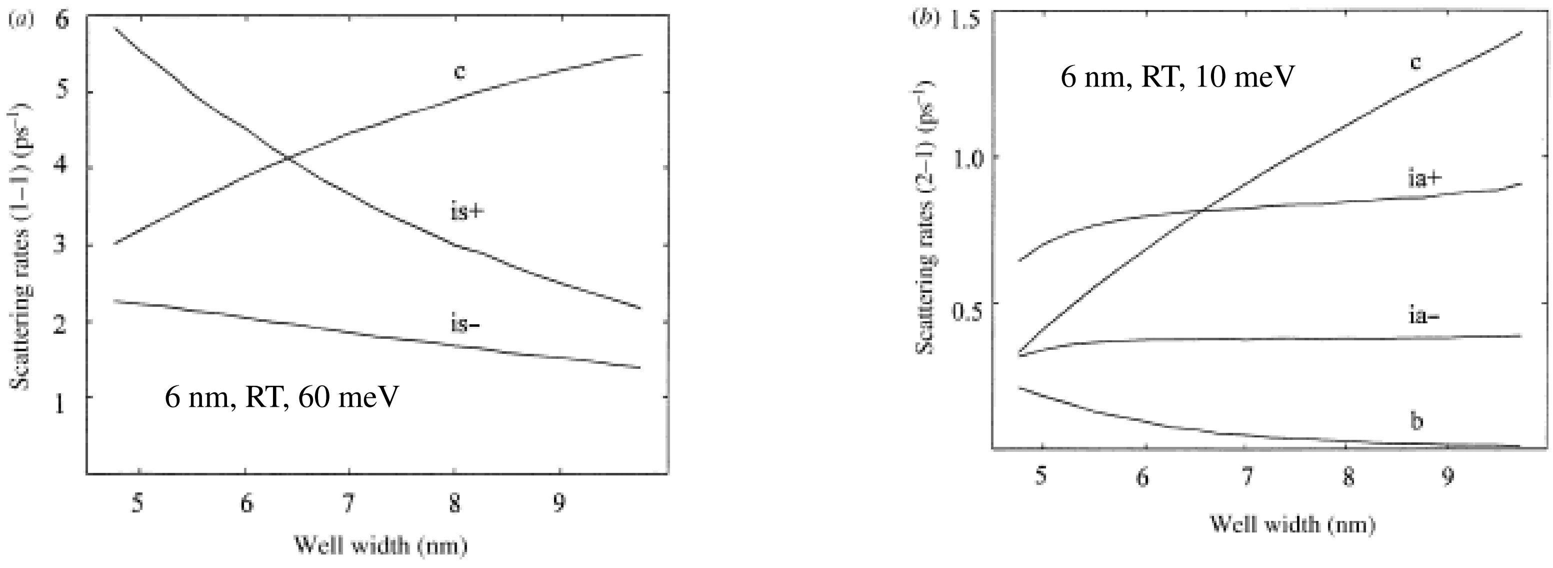

Interface-Phonon-Assisted Processes, Con’t

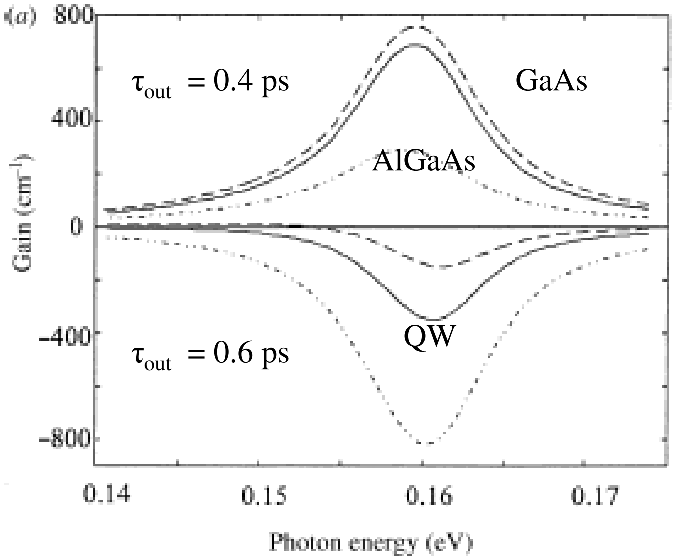

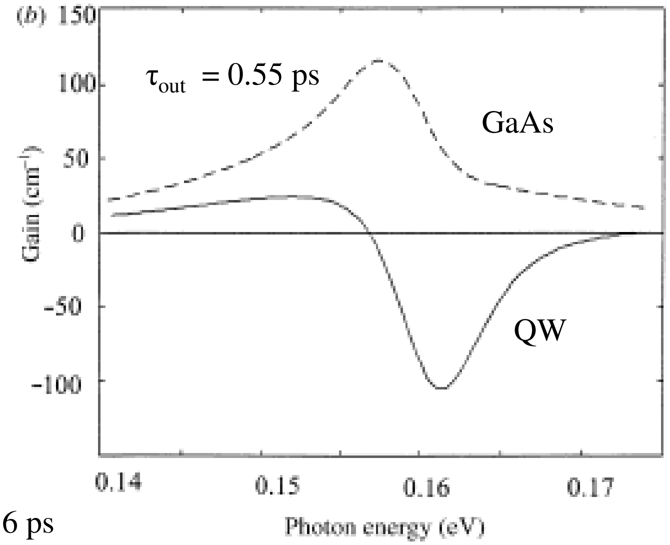

τ_{1-2} = 0.56 ps

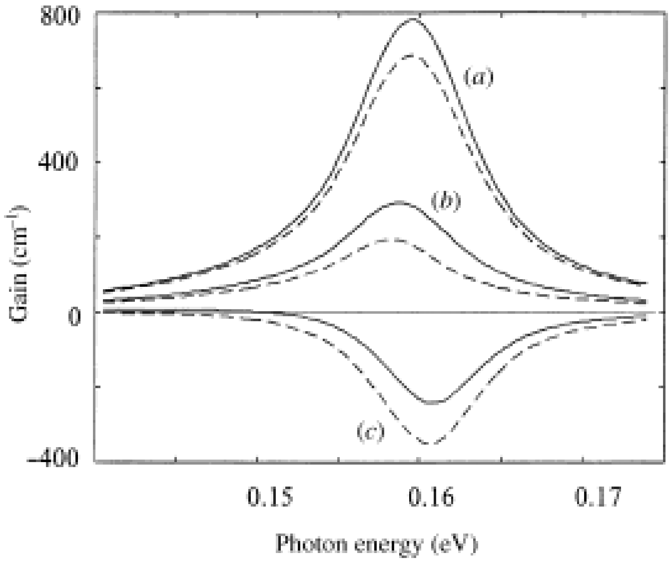

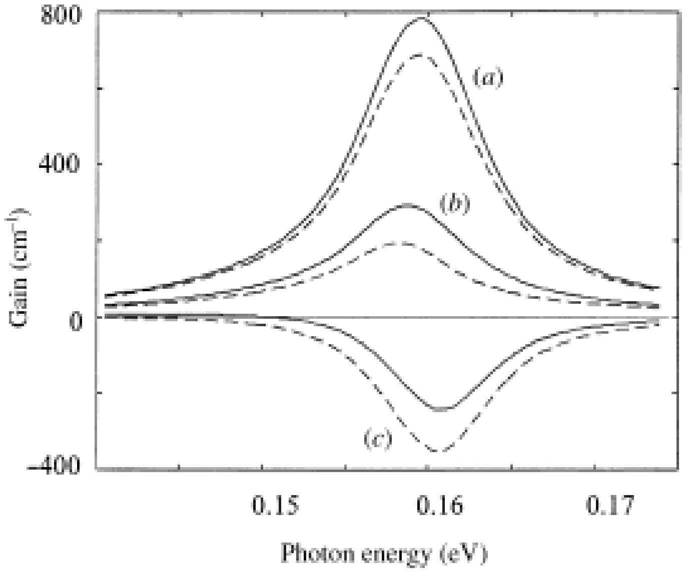

--- all modes
__ w/o barrier modes
A - 0.4 ps,
B - 0.5 ps,
C - 0.6 ps

Phonon Engineering: Some Key Techniques

- Dimensional Confinement and Boundary Effects Cause Plane Wave Phonons (Bulk Phonons) to by Replaced by Set of Modes --- Same as Putting Electromagnetic Wave in a Waveguide

- Bulk modes → Confined modes, plus interface modes, plus half-space modes with new energies, and spatial profiles.

SINCE CARRIER INTERACTIONS MUST CONSERVE ENERGY AND MOMENTUM HAVING NEW PHONON ENERGIES LEADS TO WAYS TO MODIFY CARRIER SCATTERING AND TRANSPORT…

Phonon Engineering: Some Key Techniques

EXPLOITING THE FACT THAT NEW ENERGIES LEADS TO WAYS TO MODIFY CARRIER SCATTERING AND TRANSPORT ---

- Phonon assisted transitions → Example: use to enhance population inversions in Quantum Cascade Lasers, Type-II Lasers, etc.

- Change phase space to modify interactions → In devices based on quantum wells, quantum wires, and quantum dots reduces the set of phonon momenta and energies allowed in transitions --- Example: Phase-space reductions in CNTs lead to enhanced carrier mobilities

- Modify materials to change phonons and thus interactions → Examples: (a) Form metal-semiconductor inteface to eliminate selected interface modes; (b) Reduce carrier-phonon interactions through the design of $In_xGa_{-x}N$-based structures exhibiting one mode behavior

- Modify phonon lifetimes (by arranging for different anharmonic terms) and phonon speeds (by modifying dispersion relations)→ Reduce bottleneck effects; modify thermal transport

- Generate coherent phonons using Cerenkov effect (as an example) to amplify phonon effects

Some areas where phonon engineering has clear payoff:

improved gain in semiconductor lasers (especially lasers with narrow quantum wells like quantum cascade lasers),

enhance gain in Sb-lased lasers,

coherent phonon sources for non-charge-based binary switches and devices,

increasing carrier mobilities in CNTs,

improving CNT-based IR detectors based on understand phonon-assisted non-radiative recombination,

improving III-nitride-based device performance,

phonon engineering to modify thermal conductivity.

Interface-Phonon-Assisted Processes: Enhanced Population Inversion

United States Patent 6,819,696 Belenky, Dutta, Kisin, Luryi, and Stroscio. November 16, 2004
United States Patent 7,310,361 Belenky, Dutta, Kisin, Luryi, and Stroscio. December 18, 2007

Intersubband semiconductor lasers with enhanced subband depopulation rate

Abstract

Intersubband semiconductor lasers (ISLs) are of great interest for mid-infrared (2-20 micron) device applications. These semiconductor devices have a wide range of applications from pollution detection and industrial monitoring to military functions. ISLs have generally encountered several problems which include slow intrawell intersubband relaxation times due to the large momentum transfer and small wave-function overlap of the initial and final electron states in interwell transitions. Overall, the ISL's of the prior art are subject to weak intersubband population inversion. The semiconductor device of the present invention provides optimal intersubband population inversion by providing a double quantum well active region in the semiconductor device. This region allows for small momentum transfer in the intersubband electron-phonon resonance with the substantial wave-function overlap characteristic of the intersubband scattering.

Inventors: **Belenky; Gregory** (Port Jefferson, NY); **Dutta; Mitra** (Wilmette, IL); **Kisin; Mikhail** (Lake Grove, NY); **Luryi; Serge** (Setanket, NY); **Stroscio; Michael** (Wilmette, IL) Assignee: **The United States of America as represented by the Secretary of the Army** (Washington, DC) Appl. No.: **957531** Filed: **September 21, 2001**

Resonant phonon-assisted depopulation in type-I and type-II intersubband laser heterostructures

M. V. Kisin[1], M. A. Stroscio[2], G. Belenky[1], and S. Luryi[1]

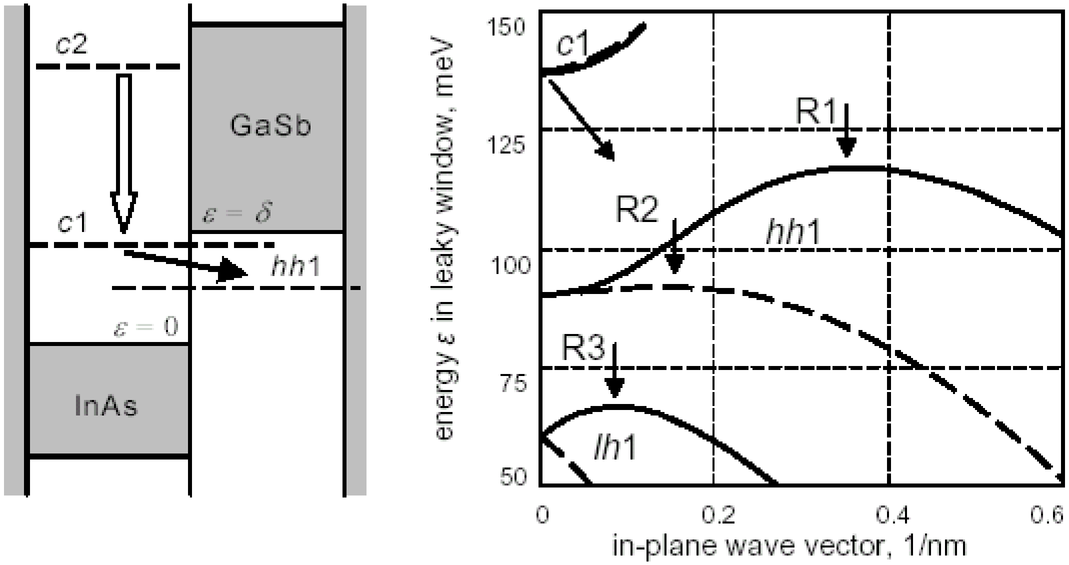

Figure 1. Left: schematic band diagram of an asymmetric InAs/GaSb DQW modeling an active region of intersubband type-II cascade laser. Black arrow depicts the interband LO-phonon assisted depopulation process. Right: subband splitting in the upper part of the leaky window δ. Short vertical arrows indicate the positions of the Van Hove singularities.

In conclusion, we show that in type-II intersubband laser heterostructures the interband LO-phonon-assisted scattering can be used as an efficient complementary process for the fast depopulation of the lower lasing states.

Inst. Phys. Conf. Ser. No 174: Section 5
Paper presented at 29th Int. Symp. Compound Semiconductors, Lausanne, Switzerland, 7-10 October 2002

Phonon-Assisted Transitions in Heterostructure Lasers

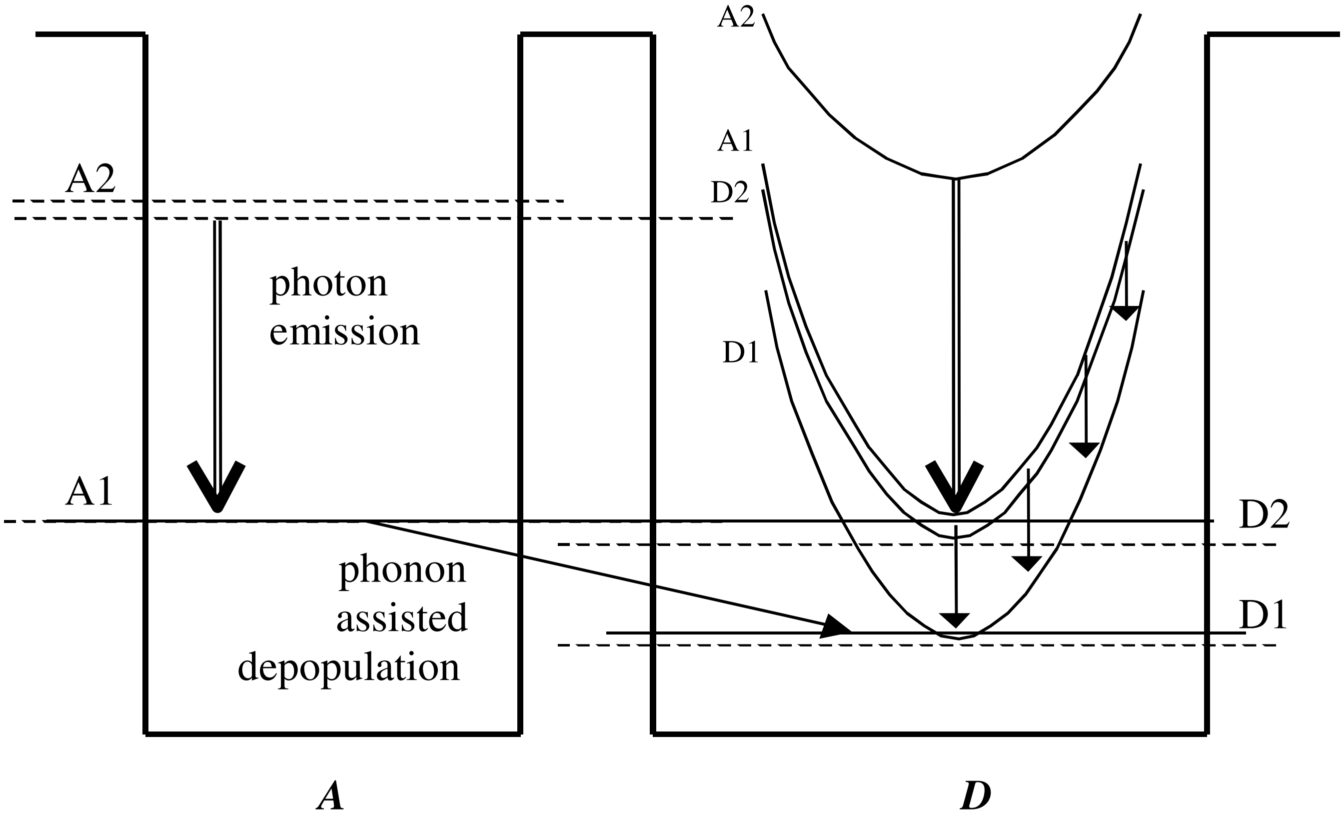

Interface-Phonon-Assisted Processes: Double Resonance Process

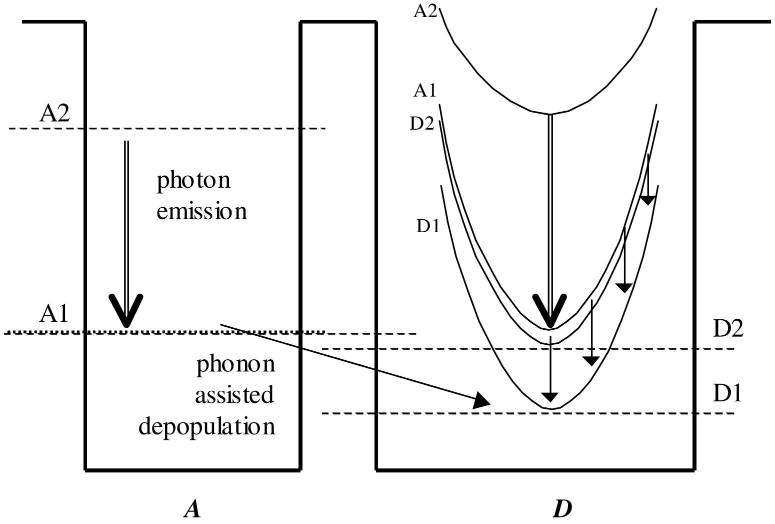

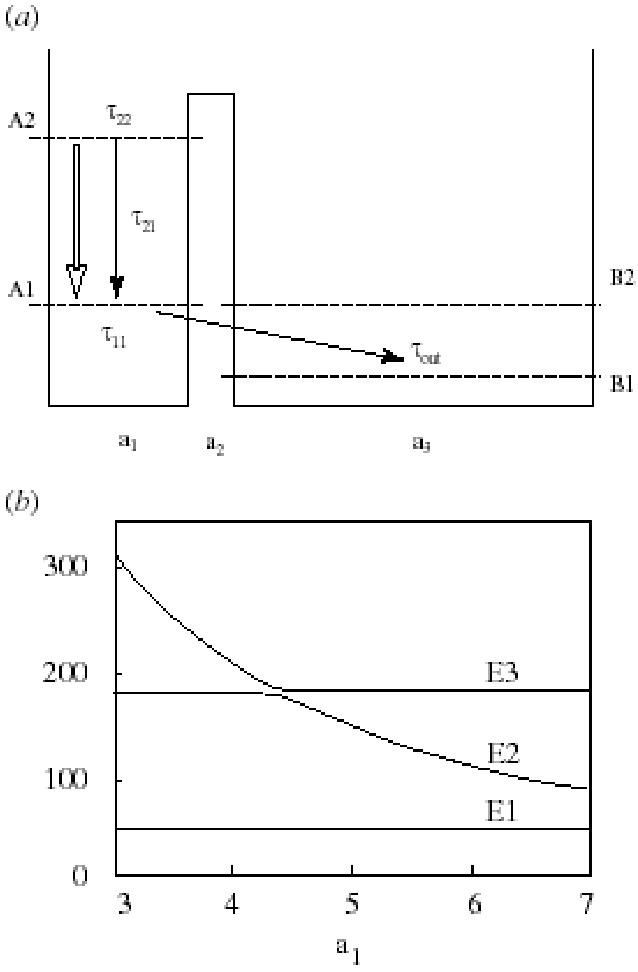

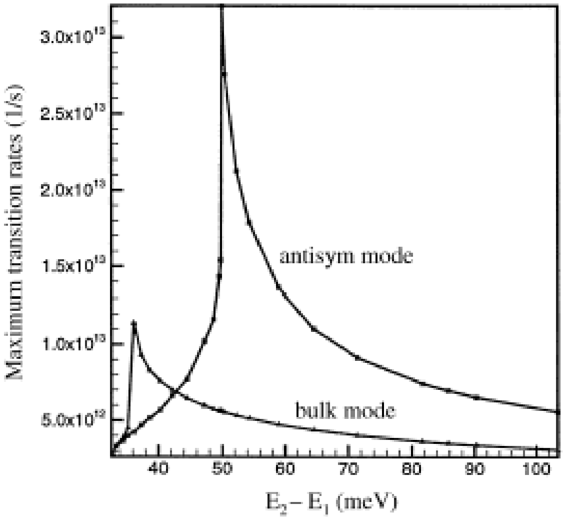

References 1-9

Interface-Phonon-Assisted Processes

1. M. Dutta, H. L. Grubin, G. J. Iafrate, K. W. Kim and M. A. Stroscio, Metal-Encapsulated Quantum Wire for Enhanced Charge Transport, CECOM Docket Number 4734, disclosed September 1991; filed September 15, 1992 (Serial No. 07/945040); Patent No. 5,264,711 issued November 23, 1993.

2. Michael A. Stroscio, Interface-Phonon--Assisted Transitions in Quantum Well Lasers, JAP, 80, 6864 (1996). --- Strong interaction of interface modes pointed out.

3. SeGi Yu, K. W. Kim, Michael A. Stroscio, G. J. Iafrate, J.-P. Sun, and G. I. Haddad, Transfer Matrix Technique for Interface Optical Phonon Modes in Multiple Quantum Well Systems, JAP, 82 3363 (1997).

4. M. Kisin, M. Stroscio, V. Gorfinkel, G. Belenky and S. Luryi, Influence of Complex Phonon Spectrum of Heterostructure on Gain Lineshape in Quantun Cascade Laser (QCL), Optical Society of America, Technical Digest Series, Volume 11, 425 (1997).

5. Mikhail V. Kisin, Vera B. Gorfinkel, Michael A. Stroscio, Gregory Belenky, and Serge Luryi, Influence of Complex Phonon Spectra on Intersubband Optical Gain, J. Appl. Phys., 82, 2031 (1997).

6. Mitra Dutta and Michael A. Stroscio, Comment on Energy Level Schemes for Far-Infrared Quantum Well Lasers, Appl. Phys. Lett., 74, 2555 (1999).

7. Michael A. Stroscio, Mikhail V. Kisin, Gregory Belenky, and Serge Luryi, Phonon Enhanced Inverse Population in Asymmetric Double Quantum Wells, Applied Physics Letters, 75, 3258 (1999).

8. J. P. Sun, G. I. Haddad, Mitra Dutta, and Michael A. Stroscio, Quantum Well Intersubband Lasers, International Journal of High Speed Electronic Systems, 9, 281 (1998).

9. Gregory Belenky, Mitra Dutta, Mikhail Kisin, Serge Luryi, and Michael Stroscio, Intersubband Semiconductor Lasers with Enhanced Subband Depopulation Rate, invention disclosure filed November 2001;
U.S. Patent No. 6,819,696, November 16, 2004.

Interface-Phonon-Assisted Processes: Applications

1. M. Dutta, H. L. Grubin, G. J. Iafrate, K. W. Kim and M. A. Stroscio, Metal-Encapsulated Quantum Wire for Enhanced Charge Transport, CECOM Docket Number 4734, disclosed September 1991; filed September 15, 1992 (Serial No. 07/945040); Patent No. 5,264,711 issued November 23, 1993.
2. Michael A. Stroscio, Interface-Phonon--Assisted Transitions in Quantum Well Lasers, JAP, 80, 6864 (1996).
5. Mikhail V. Kisin, Vera B. Gorfinkel, Michael A. Stroscio, Gregory Belenky, and Serge Luryi, Influence of Complex Phonon Spectra on Intersubband Optical Gain, J. Appl. Phys., 82, 2031 (1997).
6. Mitra Dutta and Michael A. Stroscio, Comment on Energy Level Schemes for Far-Infrared Quantum Well Lasers, Appl. Phys. Lett., 74, 2555 (1999).
9. Gregory Belenky, Mitra Dutta, Mikhail Kisin, Serge Luryi, and Michael Stroscio, Intersubband Semiconductor Lasers with Enhanced Subband Depopulation Rate, invention disclosure filed November 2001;
U.S. Patent No. 6,819,696, November 16, 2004.

B. S. Williams, B. Xu, Q. Hu, Narrow-linewidth Terahertz Emission from Three-level Systems, APL, 75, 2927 (1999); Refs. 2 and 5.

V. M. Menon, L. R. Ram-Mohan, W. D. Goodhue, A. J. Gatesman, A. S. Karakashian, "Role of Interface Phonons in Quantum Cascade Terahertz Emitters," Physica B, 316-317, 212-215 (2002); Ref. 6 and Yu, Kim, Stroscio, Iafrate, Sun, and Haddad, JAP, 82, 3363 (1997).

V. Spagnolo, G. Scamarcio, M. Troccoli, F, Capasso, C. Gmachl, A. M. Sergent, A. L. Hutcheson, D. L. Sivco, and A. Y. Cho, Nonequilibrium Optical Phonon Generation by Steady State Electron Transport in Quantum-Cascade Lasers, APL, 80, 4303-4305 (2002); Ref. 2 and Komirenko papers on nonequilibrium phonons (APL, 77, 4178 (2000) and PRB, 63, 165308, (2000).

Mariano Troccoli, Alexey Belyanin, Federico Capasso, Ertugrul Cubukcu, Deborah L. Sivco, and Alfred Y. Cho, Raman Injection Laser, Nature, 433, 845-848 (2005).

Implemented in QCL-like Heterostructure

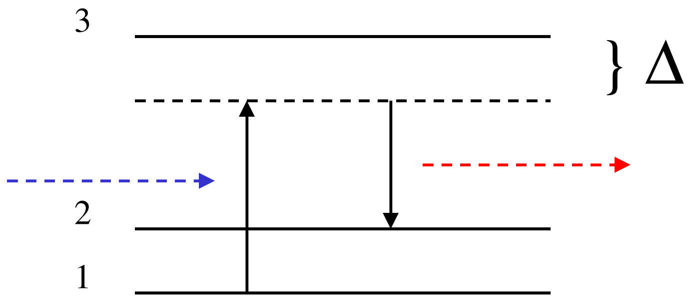

Interface-Phonon-Assisted Processes: Enhanced Population Inversion

United States Patent 6,819,696 Belenky, Dutta, Kisin, Luryi, and Stroscio. November 16, 2004
United States Patent 7,310,361 Belenky, Dutta, Kisin, Luryi, and Stroscio. December 18, 2007

Intersubband semiconductor lasers with enhanced subband depopulation rate

Abstract

Intersubband semiconductor lasers (ISLs) are of great interest for mid-infrared (2-20 micron) device applications. These semiconductor devices have a wide range of applications from pollution detection and industrial monitoring to military functions. ISLs have generally encountered several problems which include slow intrawell intersubband relaxation times due to the large momentum transfer and small wave-function overlap of the initial and final electron states in interwell transitions. Overall, the ISL's of the prior art are subject to weak intersubband population inversion. The semiconductor device of the present invention provides optimal intersubband population inversion by providing a double quantum well active region in the semiconductor device. This region allows for small momentum transfer in the intersubband electron-phonon resonance with the substantial wave-function overlap characteristic of the intersubband scattering.

Inventors: **Belenky; Gregory** (Port Jefferson, NY); **Dutta; Mitra** (Wilmette, IL); **Kisin; Mikhail** (Lake Grove, NY); **Luryi; Serge** (Setanket, NY); **Stroscio; Michael** (Wilmette, IL) Assignee: **The United States of America as represented by the Secretary of the Army** (Washington, DC) Appl. No.: **957531** Filed: **September 21, 2001**

Interface Phonon-assisted Transitions in Reduced Noise Single-Well--Double-Well Photodetectors

Design

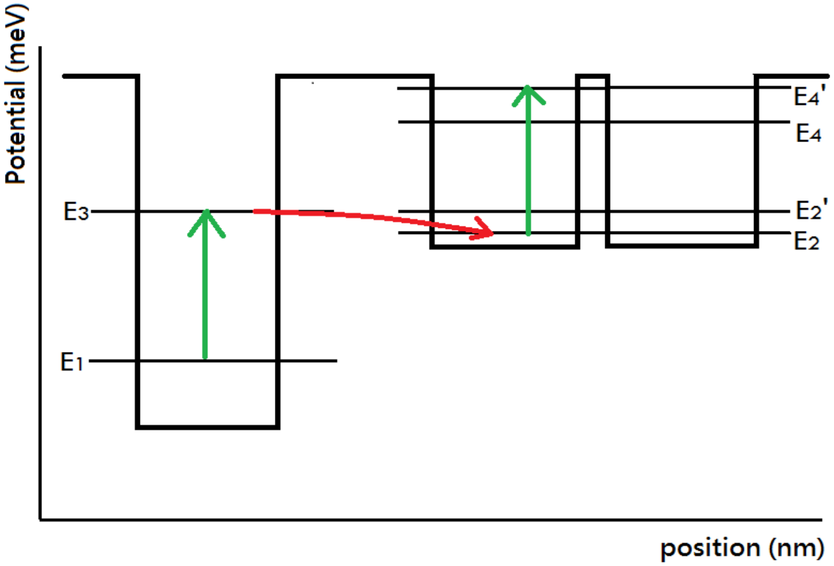

$$E_3=E_2'$$

$$E_3-E_1=E_4'-E_2=E_{photon}$$

$$E_2'-E_2=E_{\ phonon}$$

E_1 is the first energy level of the single well, and E_3 is the second energy level of it. At the meanwhile, E_2, E_2', E_4, and E_4' represent the first, second, third, and forth energy level for the double quantum well

Phonon Potential

Let the phonon potentials (Φ) for the given structure be defined as follow:

$$\begin{cases} \Phi = Ae^{qz} & \text{when } z < 0 \\ \Phi = Be^{qz} + Ce^{-qz} & \text{When } 0 \leq z < d_1 \\ \Phi = De^{q(z-d_1)} + Ee^{-q(z-d_1)} & \text{when } d_1 \leq z < d_2 \\ \Phi = Fe^{q(z-d_2)} + Ge^{-q(z-d_2)} & \text{when } d_2 \leq z < d_3 \\ \Phi = He^{q(z-d_3)} + Ie^{-q(z-d_3)} & \text{when } d_3 \leq z < d_4 \\ \Phi = Je^{q(z-d_4)} + Ke^{-q(z-d_4)} & \text{when } d_4 \leq z < d_5 \\ \Phi = e^{-q(z-d_5)} & \text{when } z \geq d_5 \end{cases} \qquad (1)$$

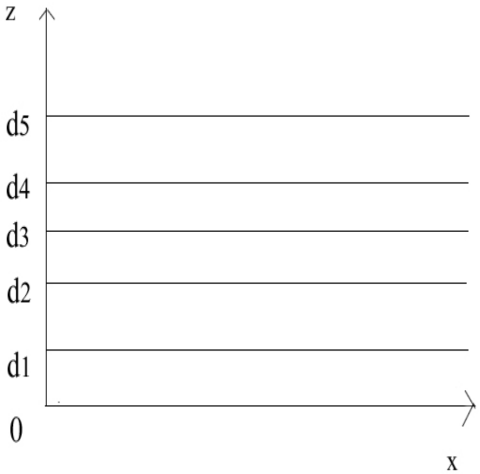

A, B, C, D, E, F, G H, I, J and K are constants in the potential equations.

At the heterointerface of region 1 and region 2, the dielectric function of the semiconductor in the structure under study is ε, then the following two condition have to be satisfied:

$$\Phi_1(Z) = \Phi_2(Z) \qquad \varepsilon_1 \frac{\partial \Phi_1}{\partial z} = \varepsilon_2 \frac{\partial \Phi_2}{\partial z} \qquad (2)$$

Phonon Potential

From the previous equations we can get the relationship between the constants:

$$
\begin{cases}
B = \frac{A}{2}(1-\frac{\varepsilon_1}{\varepsilon_2}) \\
C = \frac{A}{2}(1+\frac{\varepsilon_1}{\varepsilon_2}) \\
D = \frac{1}{2}((1+\frac{\varepsilon_1}{\varepsilon_2})Be^{qd_1} + (1-\frac{\varepsilon_1}{\varepsilon_2})Ce^{-qd_1}) \\
E = \frac{1}{2}((1-\frac{\varepsilon_1}{\varepsilon_2})Be^{qd_1} + (1+\frac{\varepsilon_1}{\varepsilon_2})Ce^{-qd_1}) \\
F = \frac{1}{2}((1+\frac{\varepsilon_1}{\varepsilon_3})De^{q(d_2-d_1)} + (1-\frac{\varepsilon_1}{\varepsilon_3})Ee^{-q(d_2-d_1)}) \\
G = \frac{1}{2}((1-\frac{\varepsilon_1}{\varepsilon_3})De^{q(d_2-d_1)} + (1+\frac{\varepsilon_1}{\varepsilon_3})Ee^{-q(d_2-d_1)})
\end{cases}
\qquad
\begin{cases}
H = \frac{1}{2}((1+\frac{\varepsilon_3}{\varepsilon_1})Fe^{q(d_3-d_2)} + (1-\frac{\varepsilon_3}{\varepsilon_1})Ge^{-q(d_3-d_2)}) \\
I = \frac{1}{2}((1-\frac{\varepsilon_3}{\varepsilon_1})Fe^{q(d_3-d_2)} + (1+\frac{\varepsilon_3}{\varepsilon_1})Ge^{-q(d_3-d_2)}) \\
J = \frac{1}{2}((1+\frac{\varepsilon_1}{\varepsilon_3})He^{q(d_4-d_3)} + (1-\frac{\varepsilon_1}{\varepsilon_3})Ie^{-q(d_4-d_3)}) \\
K = \frac{1}{2}((1-\frac{\varepsilon_1}{\varepsilon_3})He^{q(d_4-d_3)} + (1+\frac{\varepsilon_1}{\varepsilon_3})Ie^{-q(d_4-d_3)})
\end{cases}
\tag{3}
$$

And we can also get the secular equation of this system

$$
\frac{Je^{q(d_5-d_4)} + Ke^{-q(d_5-d_4)}}{Je^{q(d_5-d_4)} - Ke^{-q(d_5-d_4)}} = -\frac{\varepsilon_3}{\varepsilon_1} \tag{4}
$$

Plug the relationship between these constants into the secular equation we can then solve it to get the interface phonon modes of this system

Phonon Potential

In order to calculate the potential of this system, we need to figure out the constants in the potential equations. So here we will normalize the potential of this system to get these constants.

For cubic material, the normalization condition is given by:

$$\frac{\hbar}{2\omega L^2} = \sum \frac{1}{4\pi} \frac{1}{2\omega} \frac{\partial \varepsilon_i(\omega)}{\partial \omega} \int_{R_i} dz \left(q^2 \left| \Phi_i(q,z) \right|^2 + \left| \frac{\partial \Phi_i(q,z)}{\partial z} \right|^2 \right) \tag{5}$$

Then the normalization condition becomes:

$$\begin{aligned} &\frac{\partial \varepsilon_1(\omega)}{\partial \omega} q A^2 + \frac{\partial \varepsilon_2(\omega)}{\partial \omega} q (B^2 (e^{2qd_1} - 1) + C^2 (1 - e^{-2qd})) + \frac{\partial \varepsilon_1(\omega)}{\partial \omega} q (D^2 (e^{2q(d_2 - d_1)} - 1) + E^2 (1 - e^{-2q(d_2 - d_1)})) \\ &\frac{\partial \varepsilon_3(\omega)}{\partial \omega} q (F^2 (e^{2q(d_3 - d_2)} - 1) + G^2 (1 - e^{-2q(d_3 - d_2)})) + \frac{\partial \varepsilon_1(\omega)}{\partial \omega} q (H^2 (e^{2q(d_4 - d_3)} - 1) + I^2 (1 - e^{-2q(d_4 - d_3)})) \\ &+ \frac{\partial \varepsilon_3(\omega)}{\partial \omega} q (J^2 (e^{2q(d_5 - d_4)} - 1) + K^2 (1 - e^{-2q(d_5 - d_4)})) - \frac{\partial \varepsilon_1(\omega)}{\partial \omega} q = \frac{4\pi\hbar}{L^2} \end{aligned} \tag{6}$$

Plug the relationship between these constants into the normalization condition we can get a equation with one unknown A, then we can solve it to get constant A. As long as we know A we can calculate the rest constants.

Results

GaAlAs/GaAs material system

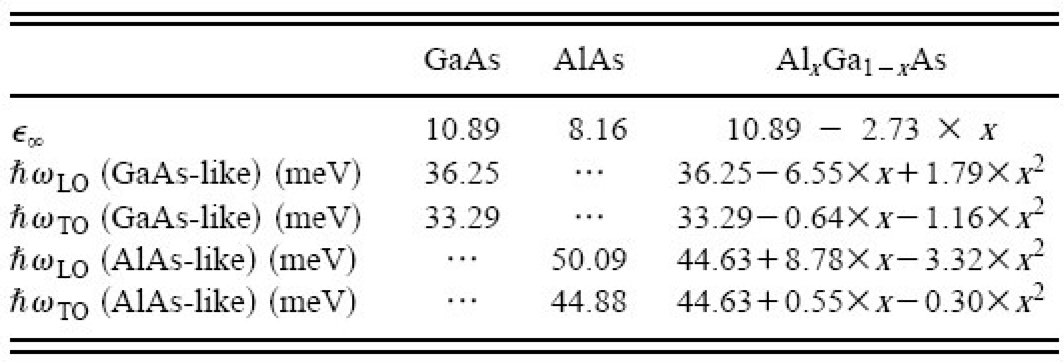

	GaAs	AlAs	$Al_xGa_{1-x}As$
ϵ_∞	10.89	8.16	$10.89 - 2.73 \times x$
$\hbar\omega_{LO}$ (GaAs-like) (meV)	36.25	⋯	$36.25 - 6.55 \times x + 1.79 \times x^2$
$\hbar\omega_{TO}$ (GaAs-like) (meV)	33.29	⋯	$33.29 - 0.64 \times x - 1.16 \times x^2$
$\hbar\omega_{LO}$ (AlAs-like) (meV)	⋯	50.09	$44.63 + 8.78 \times x - 3.32 \times x^2$
$\hbar\omega_{TO}$ (AlAs-like) (meV)	⋯	44.88	$44.63 + 0.55 \times x - 0.30 \times x^2$

SeGi Yu, K. W. Kim, Michael A. Stroscio, G. J. Lafrate, J,-P. Sun et al, JAP, 82, 3363 (1997)

We calculate the parameters we need

Phonon modes (meV)	**$Ga_{0.452}Al_{0.548}As$ (AlAs-like)**	**GaAs**	**$Ga_{0.741}Al_{0.259}As$ (GaAs-like)**
LO	48.44	36.25	34.67
TO	44.83	33.29	33.046

Results

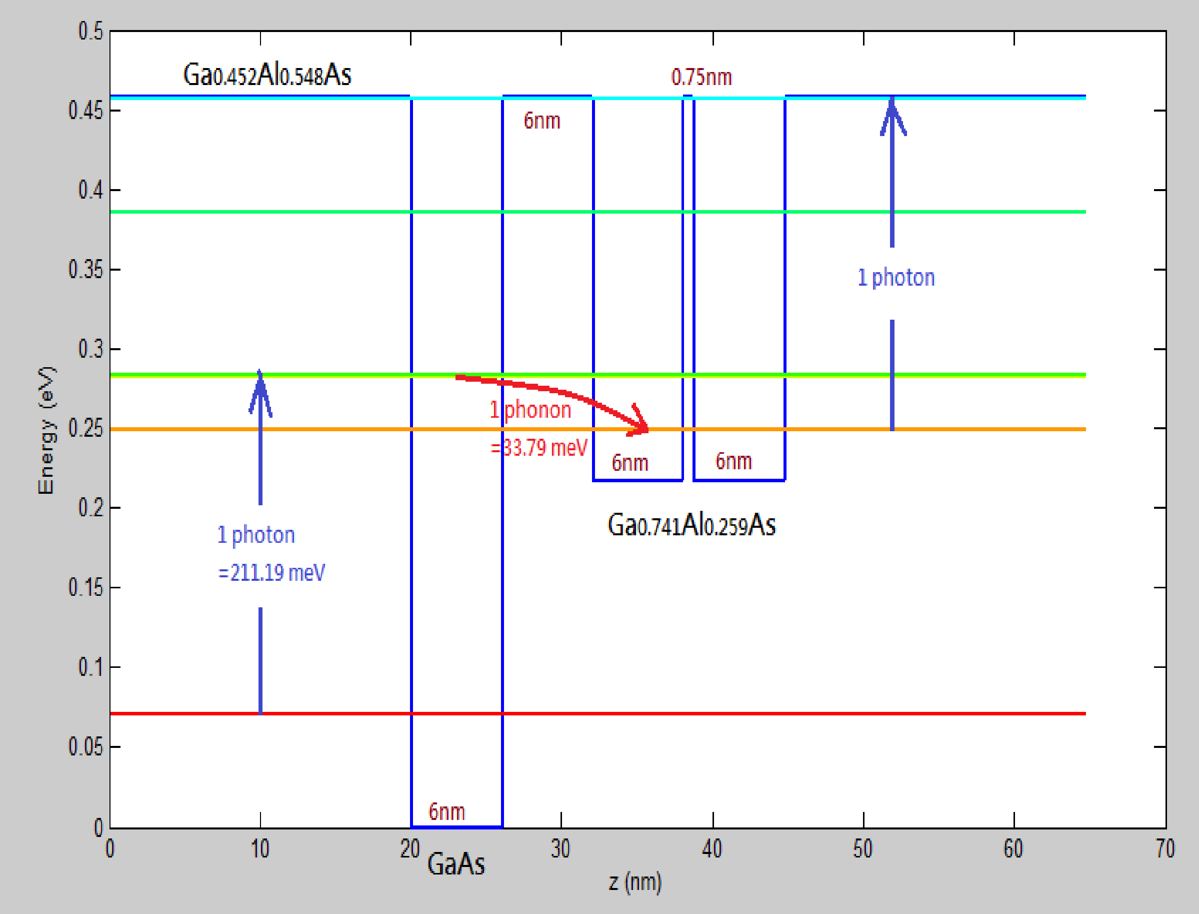

Interfaces phonon modes

at q=1e8 (wavevector)

IF Phonon modes (meV)	
33.38808	44.3023
33.8125	44.9045
34.193	46.278
34.6304	47.1212
35.57657	48.038603

Dispersion curve

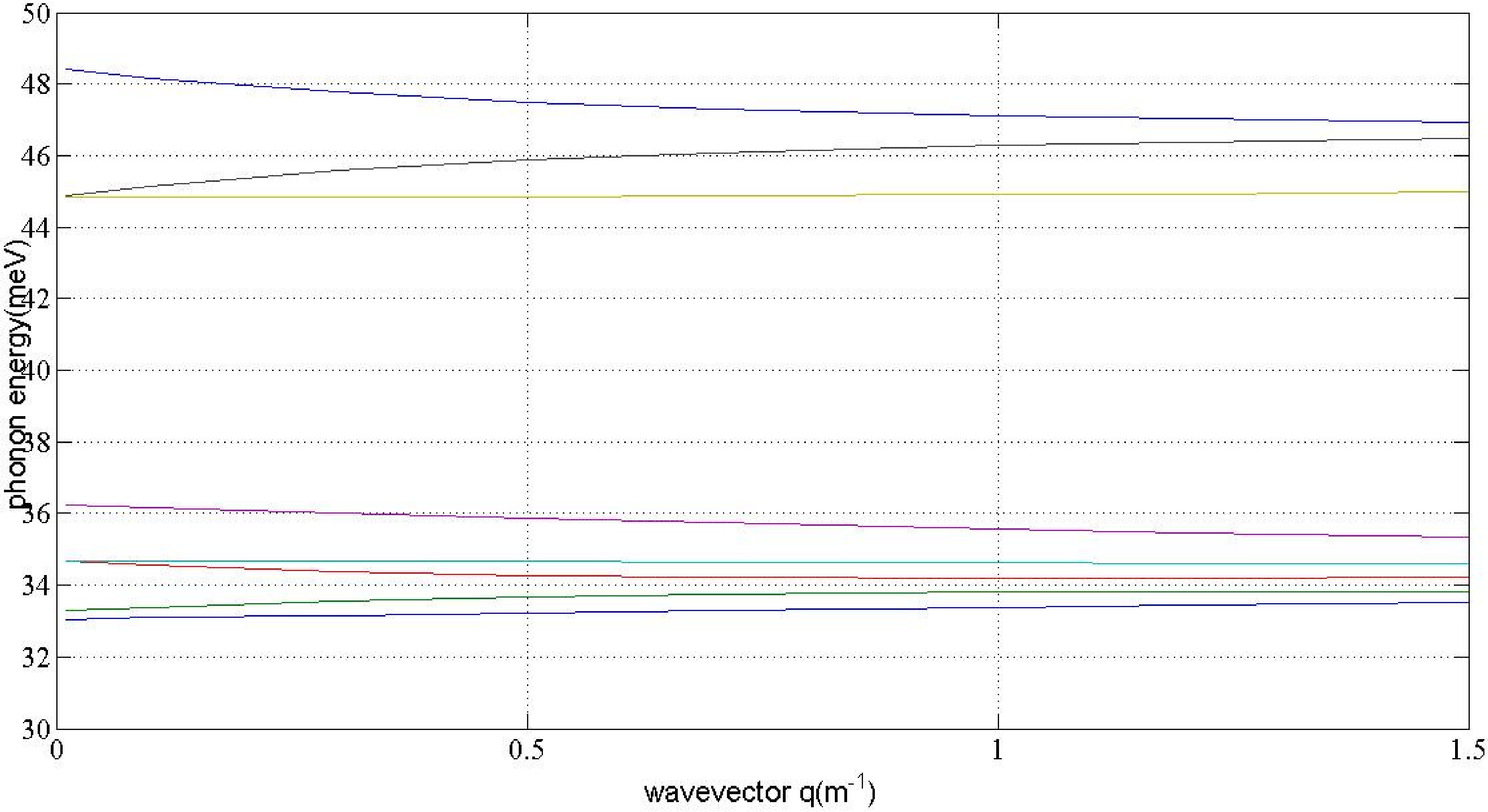

Phonon Potential

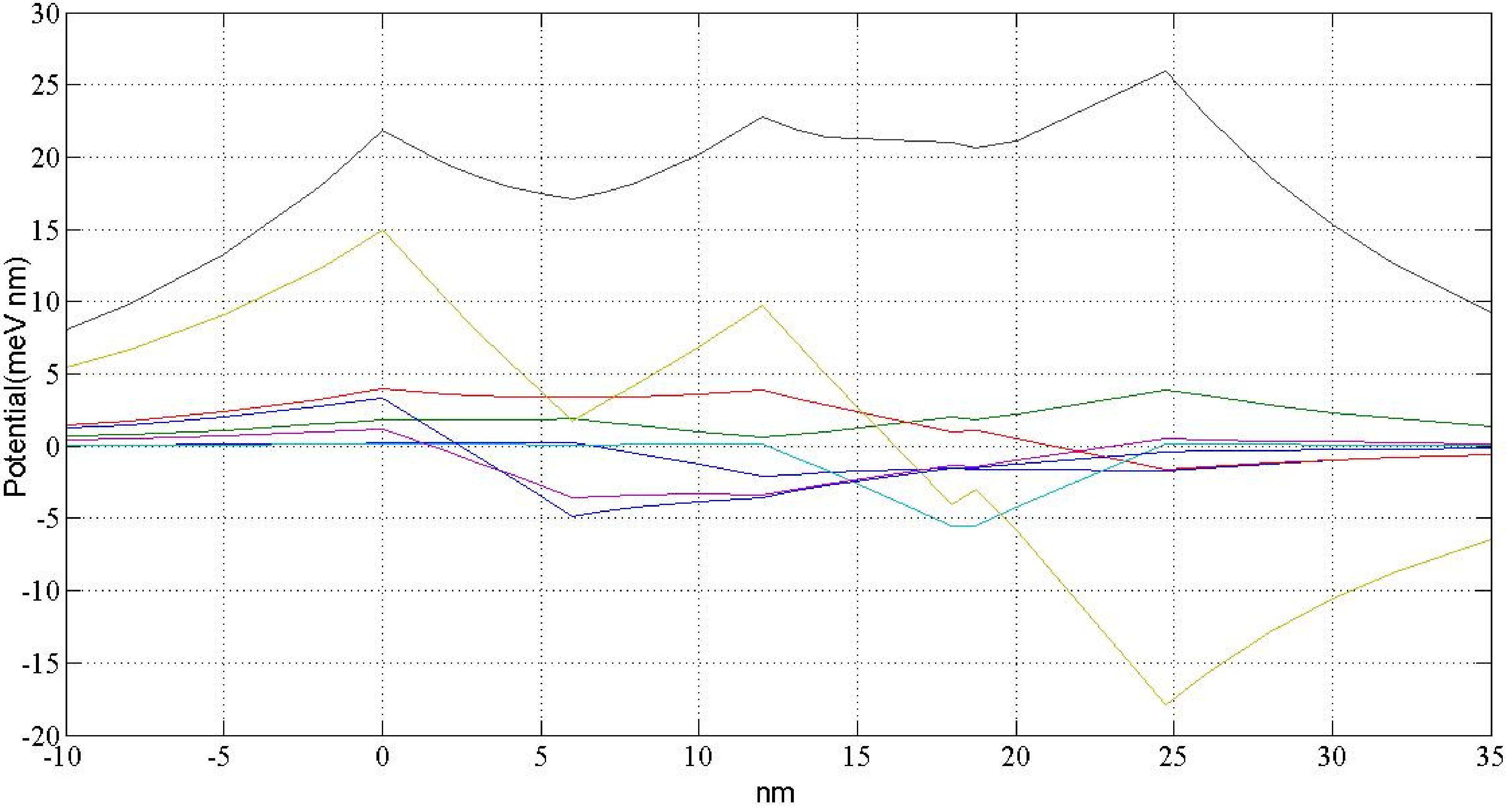

Phonon Potential

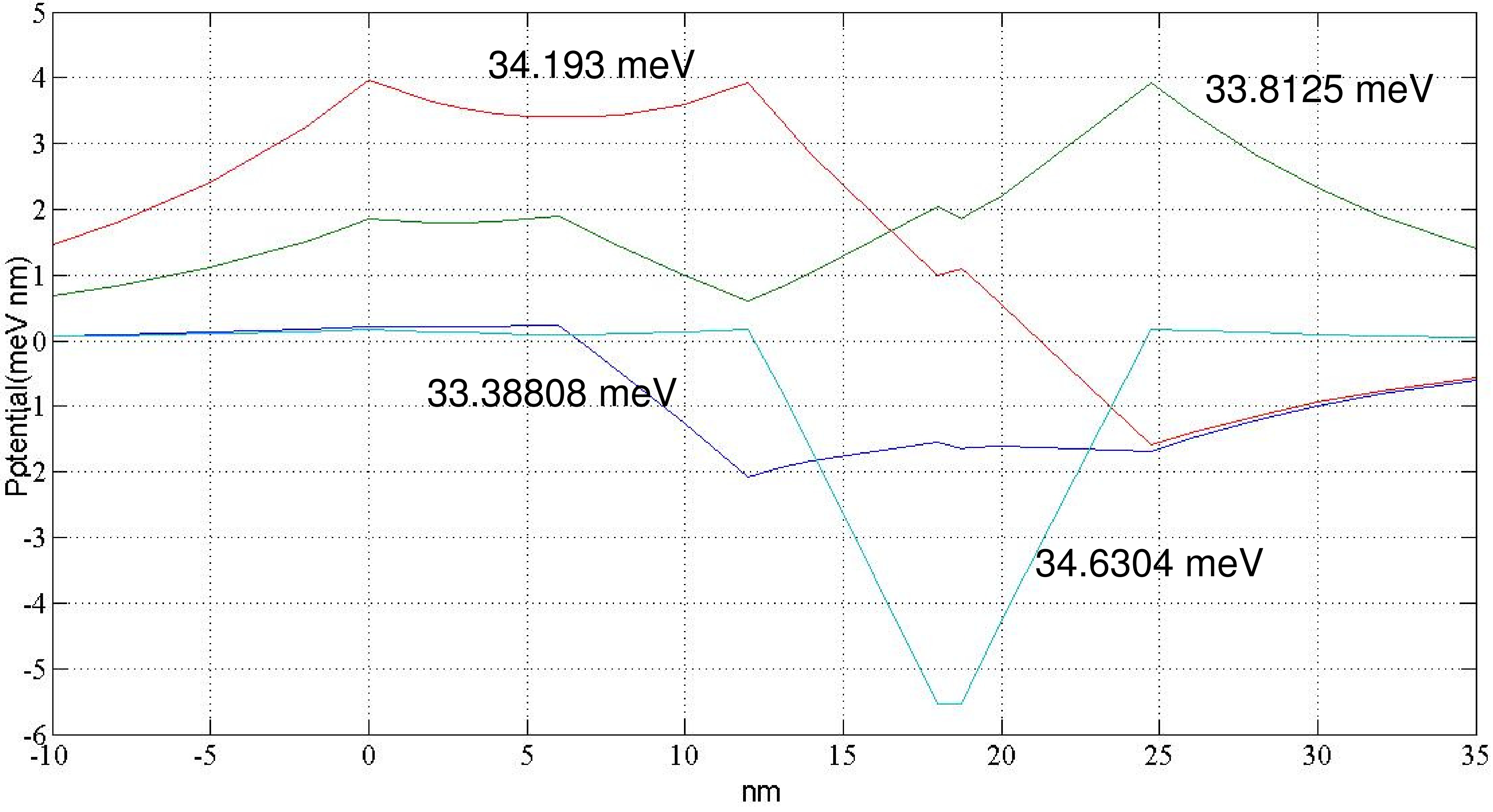

Phonon Potential

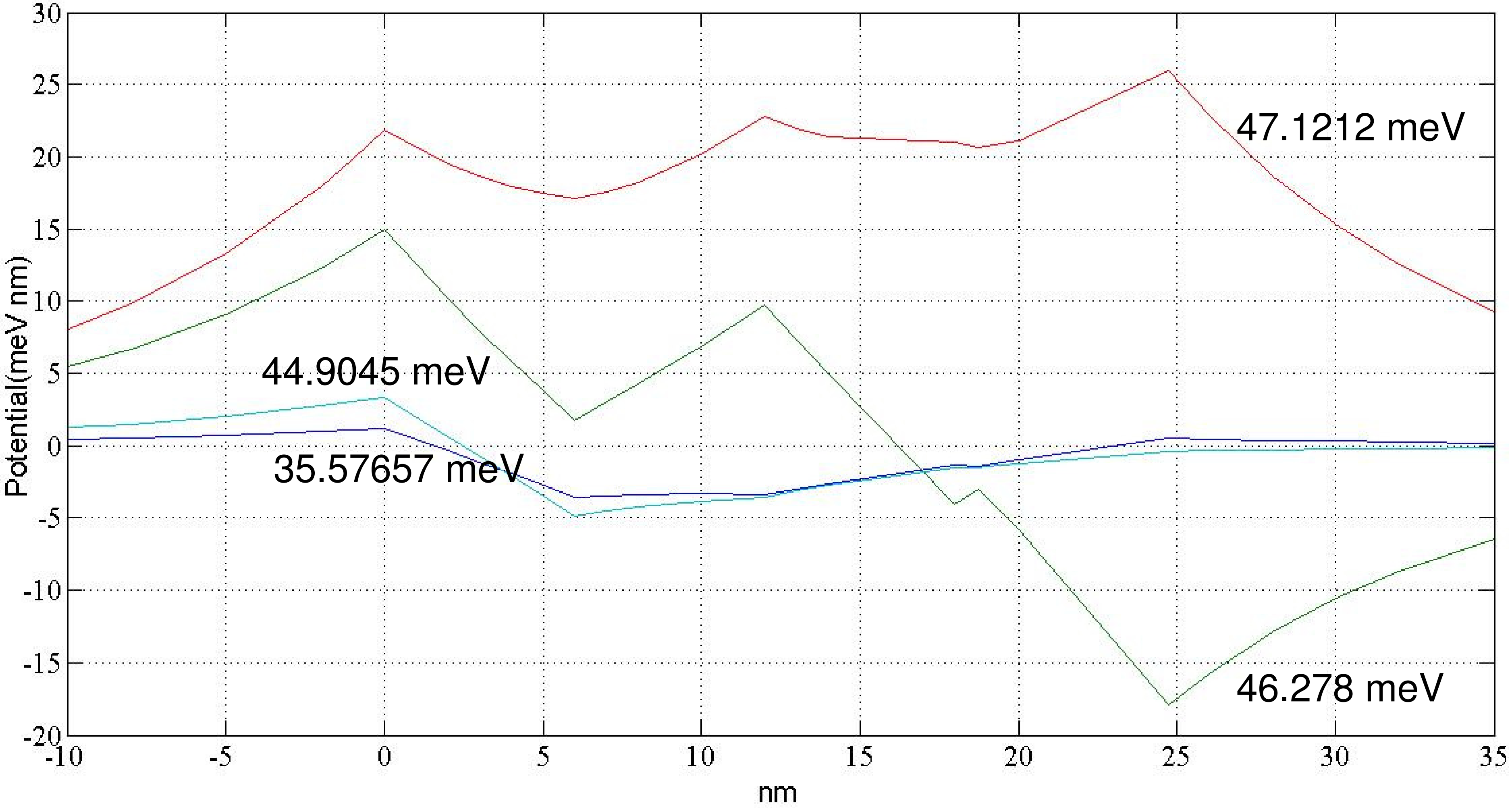

Results

InGaAs/InAs material system

For $In_xGa_{1-x}As$

InAs-like GaAs-like

$242.99 - 32.54x + 4.545x^2$ **TO** $268 - 62x + 220x^2$ **TO**

$253.97 - 67.91x + 51.94x^2$ **LO** $291 - 59.167x + 152.7789x^2$ **LO**

Then, we calculate the parameters we need

Phonon modes (meV)	**$In_{0.248}Ga_{0.752}As$**	**$In_{0.59}Ga_{0.41}As$**	**InAs**
LO	35.32	28.746	29.74
TO	32.89	27.93	27.01
ε_∞	11.526	11.287	11.7

Results

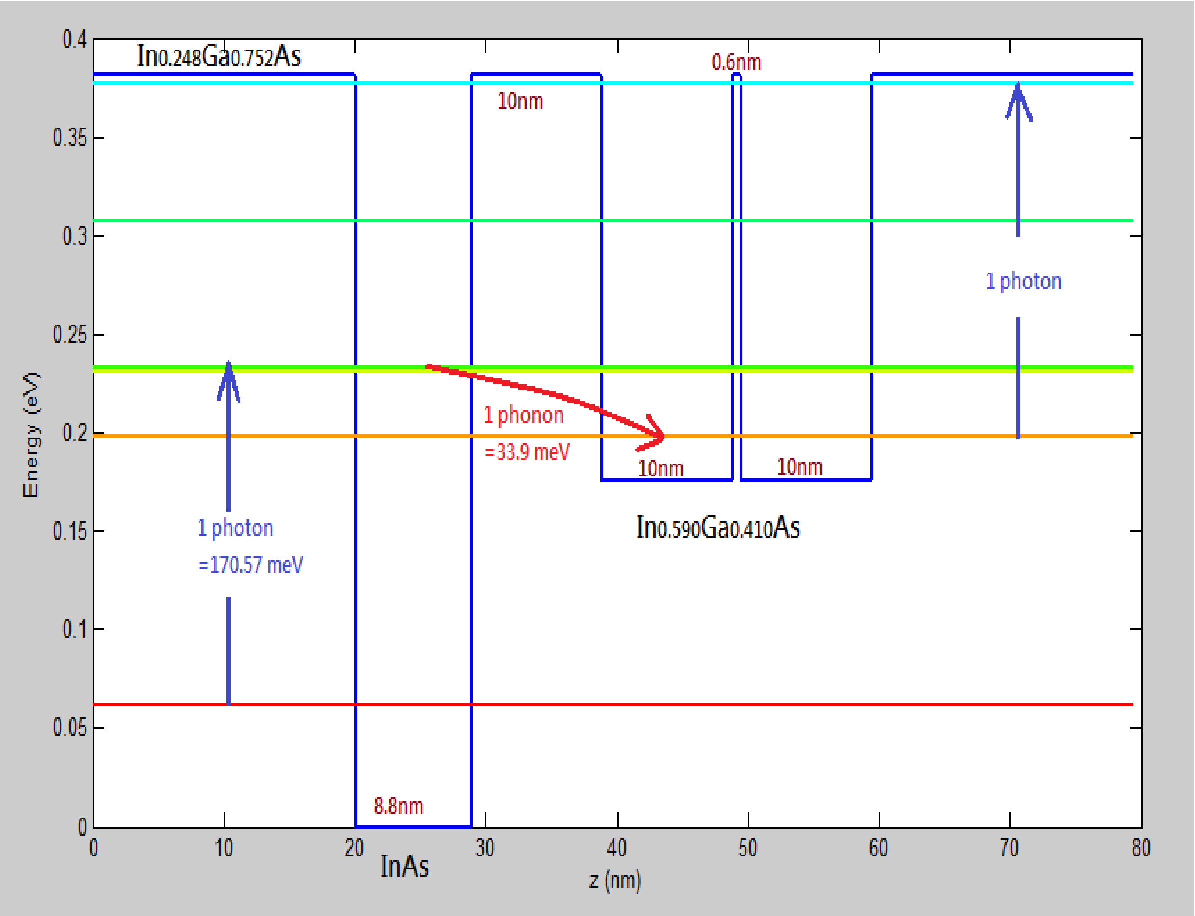

Interfaces phonon modes

at q=1e8 (wavevector)

IF Phonon modes (meV)	
29.542	33.6199006
30.351	34.72185
32.7285	35.1522

Results

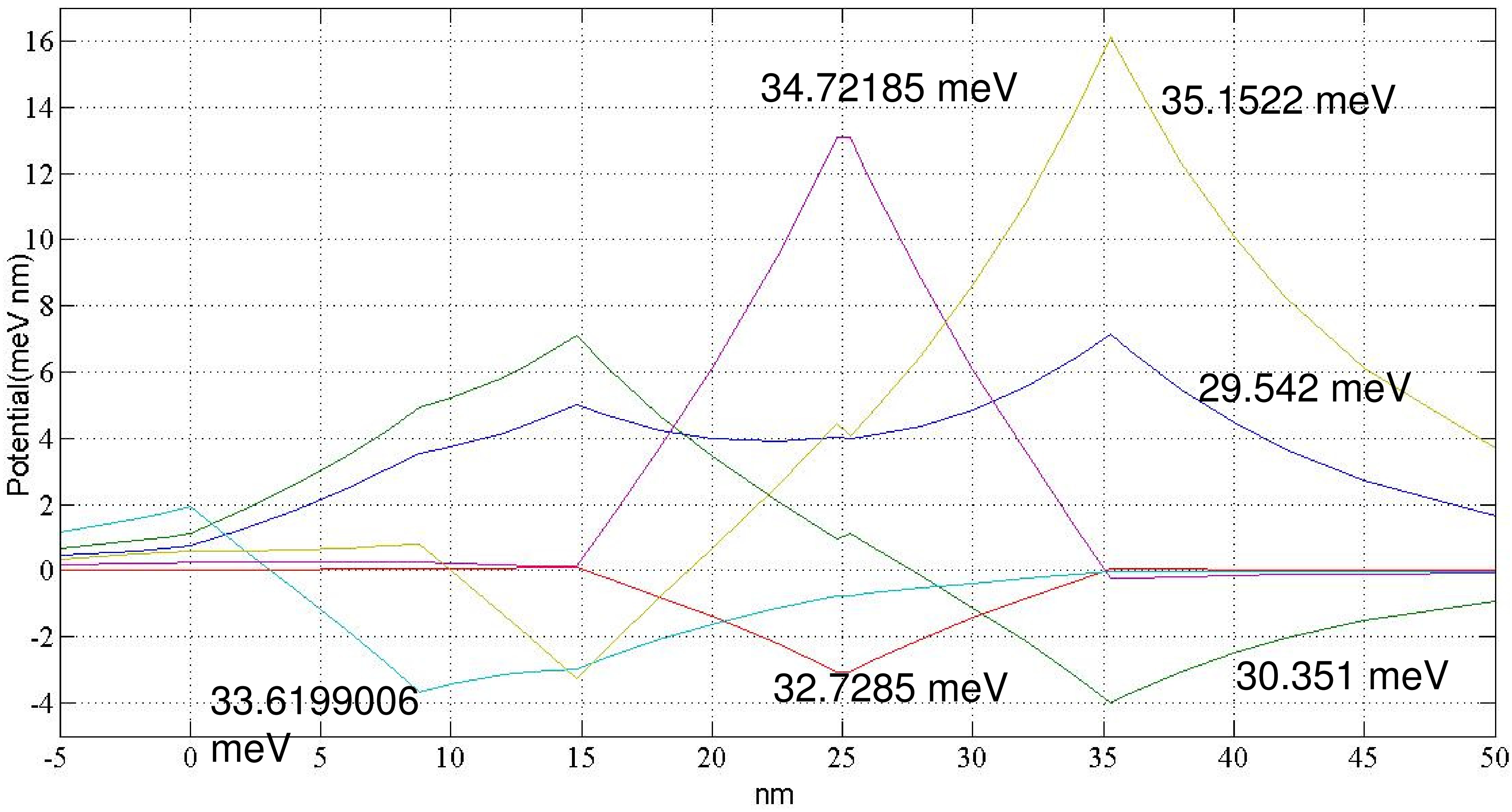
34.72185 meV
35.1522 meV
29.542 meV
32.7285 meV
30.351 meV
33.6199006 meV
Potential(meV nm)
nm
16
14
12
10
8
6
4
2
0
-2
-4
-5
0
5
10
15
20
25
30
35
40
45
50

Results

InAlAs/InP material system

For $In_xAl_{1-x}As$

AlAs-like		InAs-like	
$361.5-24x-9.5x^2$	**TO**	$229+22x-13x^2$	**LO**
$401.5-55x-20x^2$	**LO**	$229+22x-9x^2$	**TO**

Then, we calculate the parameters we need

Phonon modes (meV)	**$In_{0.36}Al_{0.64}As$**	**InP**	**$In_{0.61}Al_{0.39}As$**
LO	46.977	42.75	29.16
TO	43.57	37.63	29.23
ε_{∞}	9.4344	9.61	10.32

Results

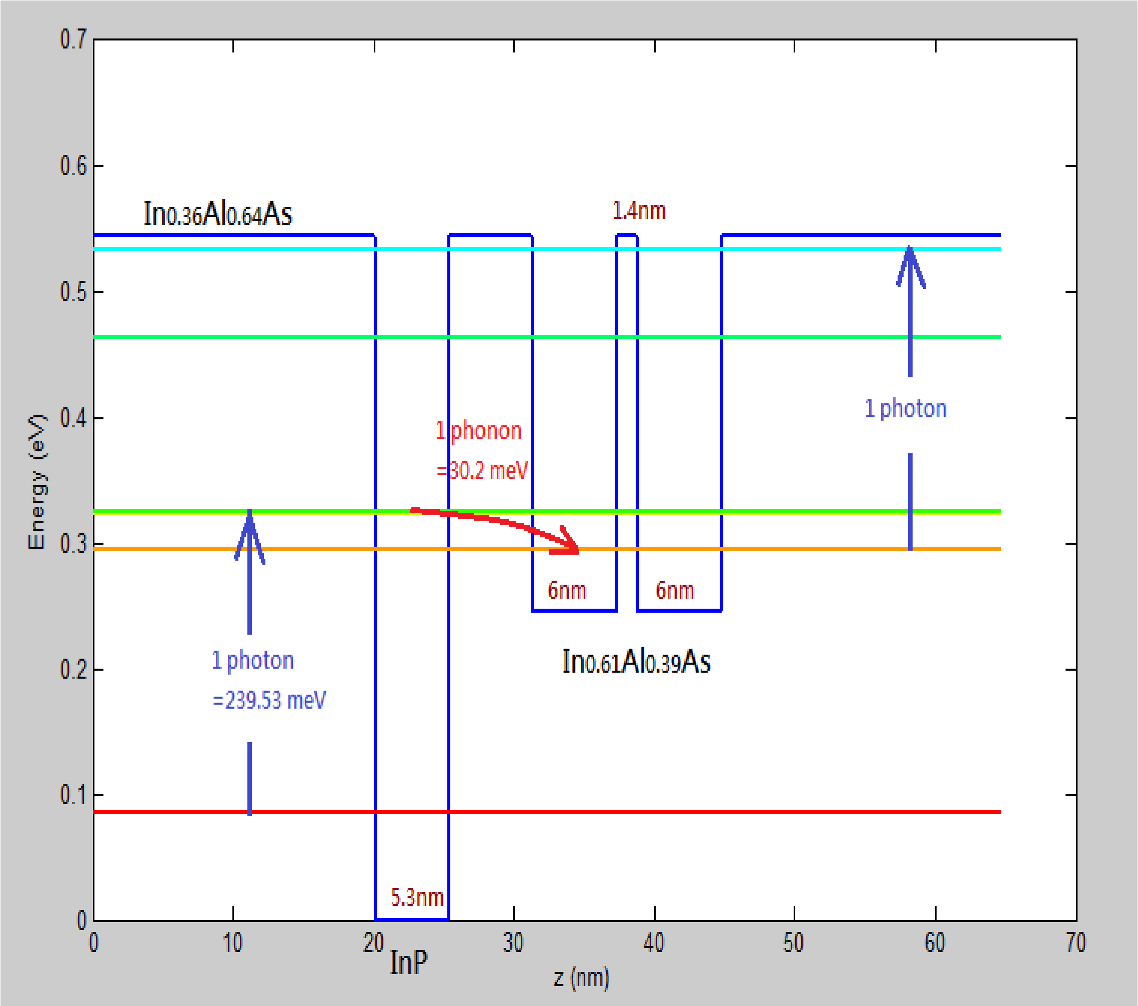

Interfaces phonon modes

at q=1e8 (wavevector)

IF Phonon modes (meV)	
29.18687	44.314
38.383165	45.15
40.99825	45.8385
43.679	

GaAlAs Design

GaAs/$Ga_{1-x}Al_xAs$

- Band Gap, $E_g=(1.426+1.247x)$ eV
- Band alignment: 33% of total discontinuity in valence band, i.e. $\Delta V_{VB}=0.33$; $\Delta V_{CB}=0.67$
- Electron effective mass, $m^*=(0.067+0.083x)m_0$

From Quantum Wells, Wires and Dots (Paul Harrison)

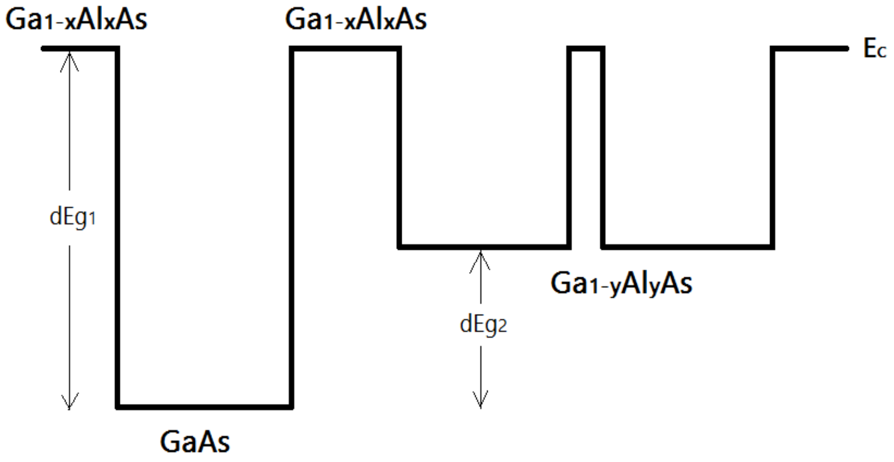

- $\mathrm{dEg}_1 = 1.247 \times \mathrm{x} \times 0.67$
- $\mathrm{dEg}_2 = 1.247 \times \mathrm{y} \times 0.67$
- $\mathrm{m}^*_{Ga_{1-x}Al_xAs} = 0.067 + 0.083 \times \mathrm{x}$
- $\mathrm{m}^*_{GaAs} = 0.067$
- $\mathrm{m}^*_{Ga_{1-y}Al_yAs} = 0.067 + 0.083 \times y$

InGaAs Design

$In_{1-x-y}Al_xGa_yAs/AlAs$

- Total band discontinuity,
  $\Delta V =$
  $[2.093x + 0.629y + 0.577x^2 + 0.436y^2 + 1.013xy - 2.0x^2(1 - x - y$
- Band alignment: 47% of total discontinuity in valence band, i.e. $\Delta VVB=0.47$; $\Delta VCB=0.53$
- Electron effective mass, $m^*=(0.0427+0.0685x)m_0$

For In1-yGayAs/AlAs,
$\Delta V = [(0.629y + 0.436y^2) \times 0.53]\ \mathrm{eV}$ **in conduction band**
Effective mass=, $m^*=(0.0427)m_0$

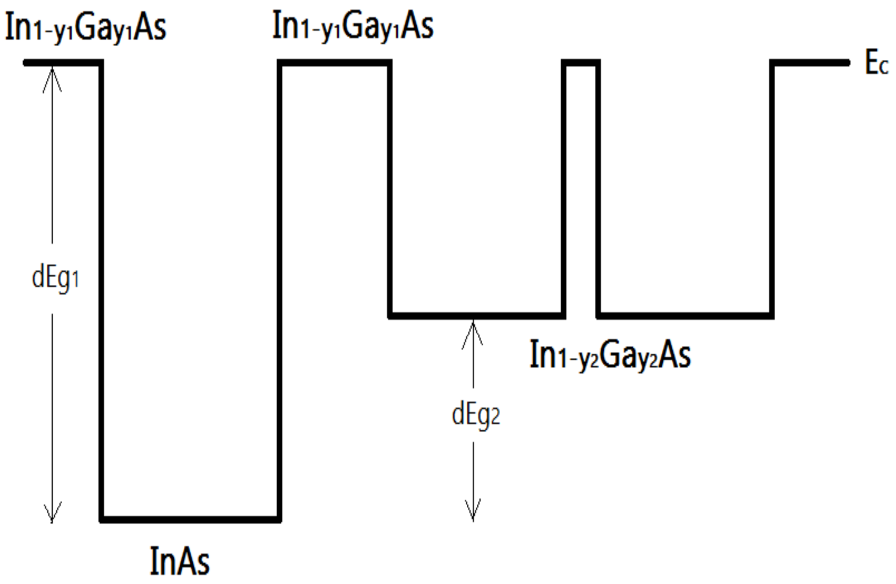

- $dEg_1 = (0.0629y_1 + 0.436y_1^2) \times 0.53$
- $dEg_2 = (0.0629y_2 + 0.436y_2^2) \times 0.53$
- $m^*_{In_{1-y_1}Ga_{y_1}As} = 0.0427$
- $m^*_{InAs} = 0.0427$
- $m^*_{In_{1-y_1}Ga_{y_1}As} = 0.0427$

InAlAs/InP Design

$In_{1-x-y}Al_xGa_yAs/AlAs$

- **Total band discontinuity,**
  $\Delta V = [2.093x + 0.629y + 0.577x^2 + 0.436y^2 + 1.013xy - 2.0x^2(1-x-y)]\ \mathrm{eV}$
- **Band alignment: 47% of total discontinuity in valence band, i.e. ΔVVB=0.47; ΔVCB=0.53**
- **Electron effective mass, $m^*=(0.0427+0.0685x)m_0$**

From Quantum Wells, Wires and Dots (Paul Harrison)

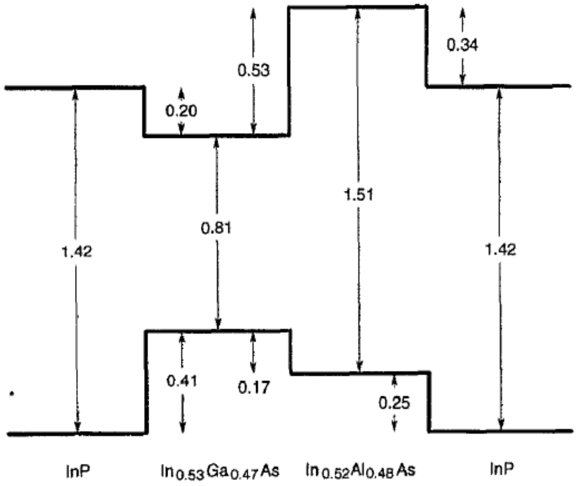

FIG. 1. Calculated valence-band offsets are combined with measured low-temperature band gaps to yield the energy band diagram (in eV) for the heterointerfaces in the $In_{0.53}Ga_{0.47}As/In_{0.52}Al_{0.48}As/InP(001)$ family.

For $In_{1-x}Al_xAs/AlAs$,
$\Delta V = [(2.093x - 1.423x^2 + 2x^3) \times 0.53]\ \mathrm{eV}$ **in conduction band**
Effective mass=, $m^*=(0.0427+0.0685x)m_0$

From Appl. Phys. Lett. Vol. 58, No. 18, 22 April 1991 (Mark S. Hybertsen)

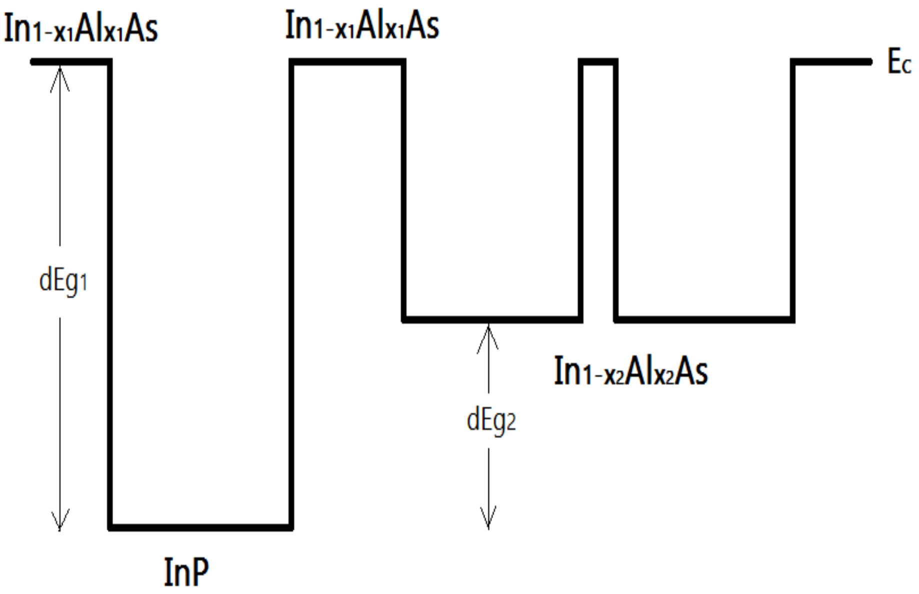

- $\mathrm{dEg}_1 = (2.093\mathrm{x}_1 - 1.423\mathrm{x}_1^2 + 2\mathrm{x}_1^3) \times 0.53 - 0.135921$
- $\mathrm{dEg}_2 = (2.093\mathrm{x}_1 - 1.423\mathrm{x}_1^2 + 2\mathrm{x}_1^3) \times 0.53 - 0.135921$
- $\mathrm{m}^*_{In_{1-x_1}Al_{x_1}As} = 0.0427 + 0.0685\mathrm{x}_1$
- $\mathrm{m}^*_{InP} = 0.08$
- $\mathrm{m}^*_{In_{1-x_2}AL_{x_2}As} = 0.0427 + 0.0685\mathrm{x}_2$

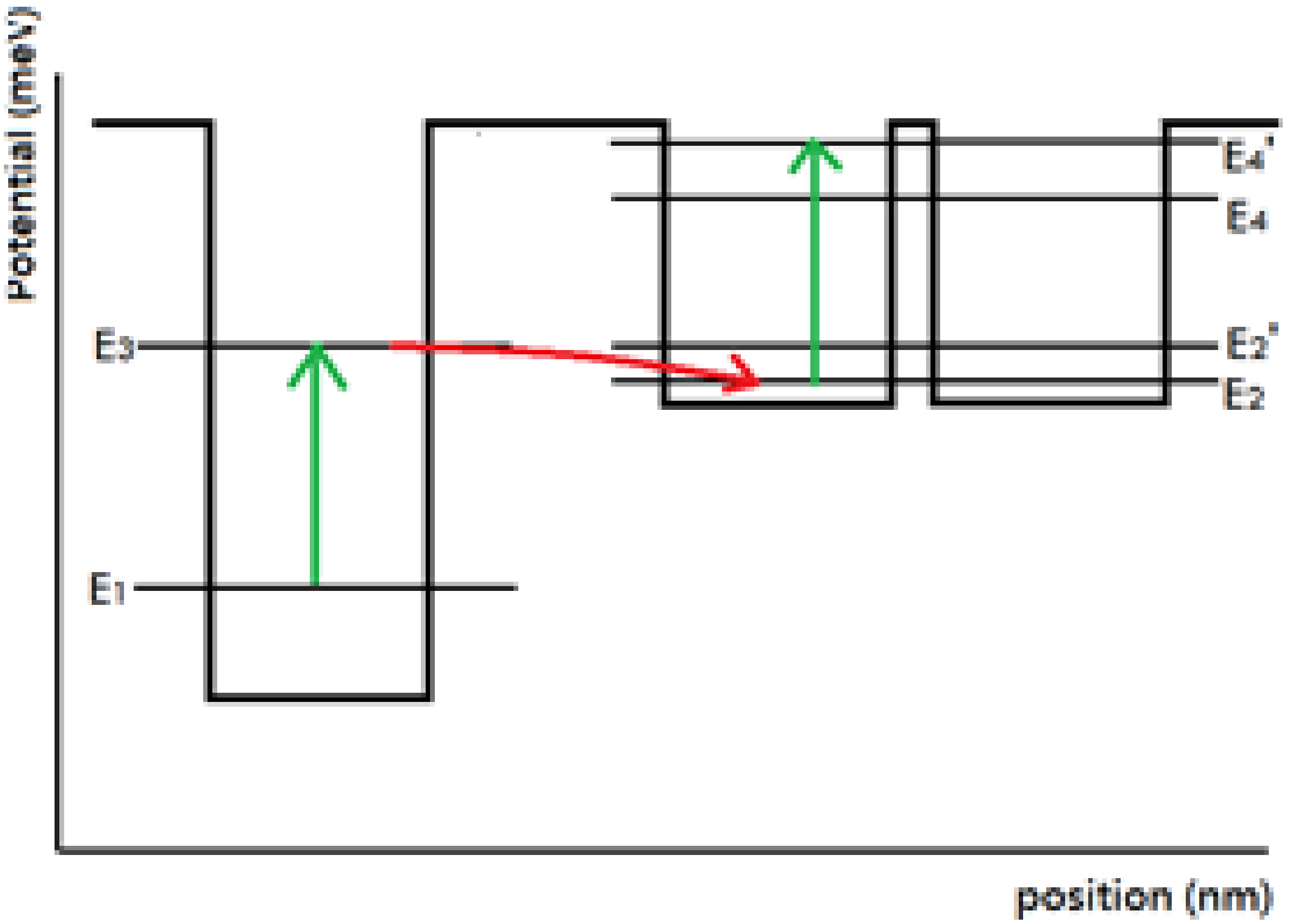
Potential (meV)
E3
E1
E4'
E4
E2'
E2
position (nm)

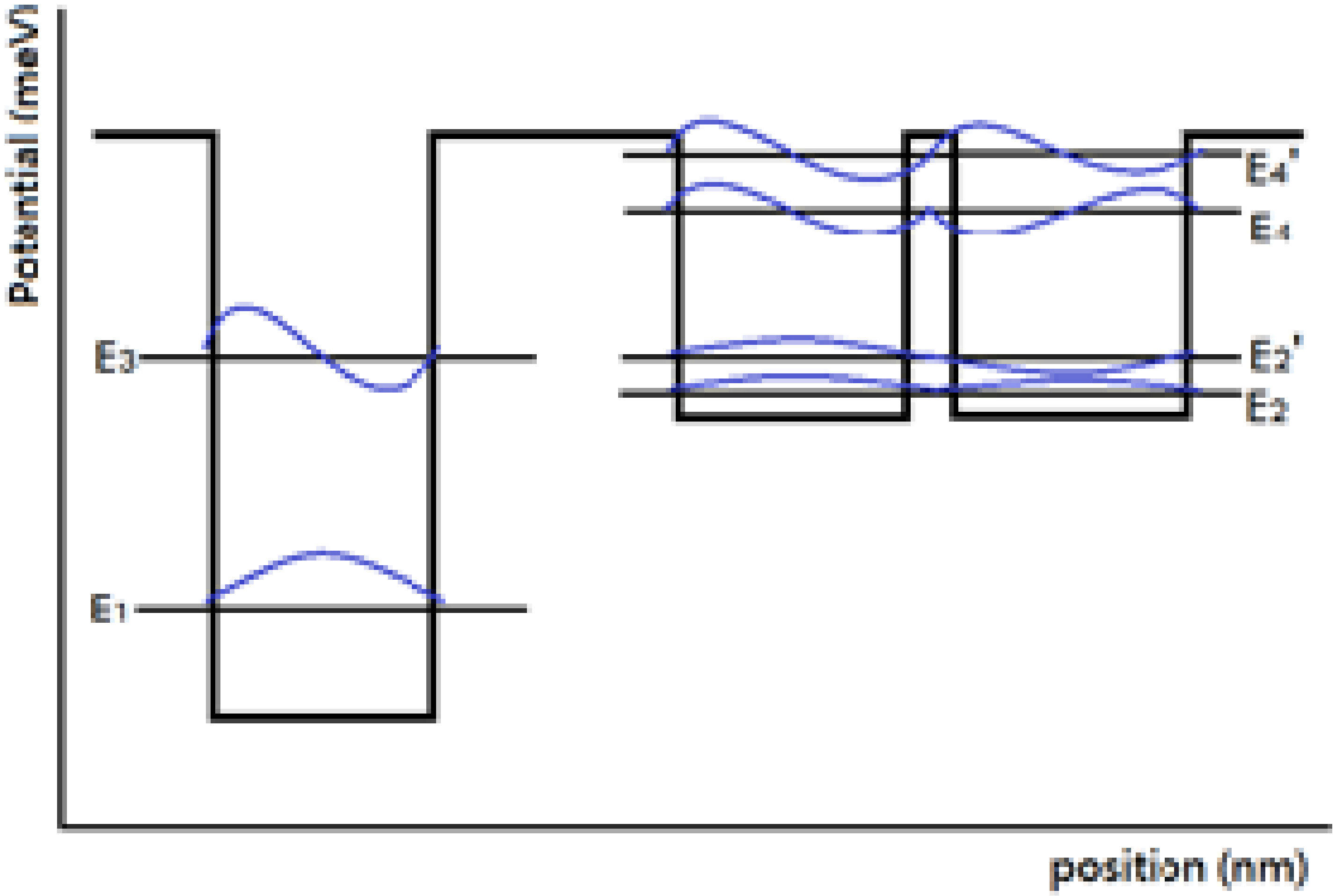
Potential (meV)
E3
E1
E4'
E4
E2'
E2
position (nm)

early

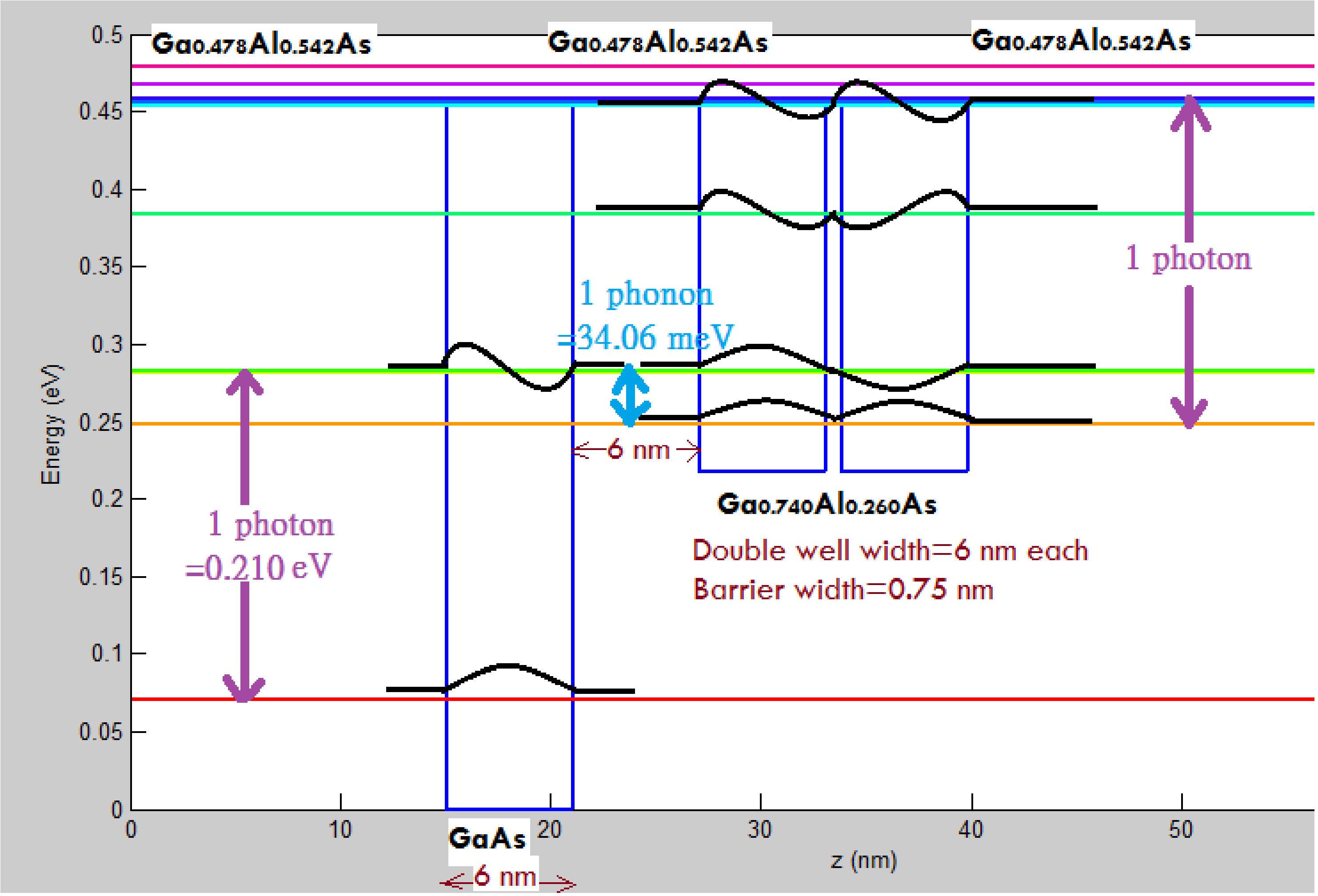
Ga0.478Al0.542As
Ga0.478Al0.542As
Ga0.478Al0.542As
1 photon
1 phonon
=34.06 meV
←6 nm→
Ga0.740Al0.260As
Double well width=6 nm each
Barrier width=0.75 nm
1 photon
=0.210 eV
Energy (eV)
0.5
0.45
0.4
0.35
0.3
0.25
0.2
0.15
0.1
0.05
0
0
10
20
30
40
50
z (nm)
GaAs
←6 nm→

early

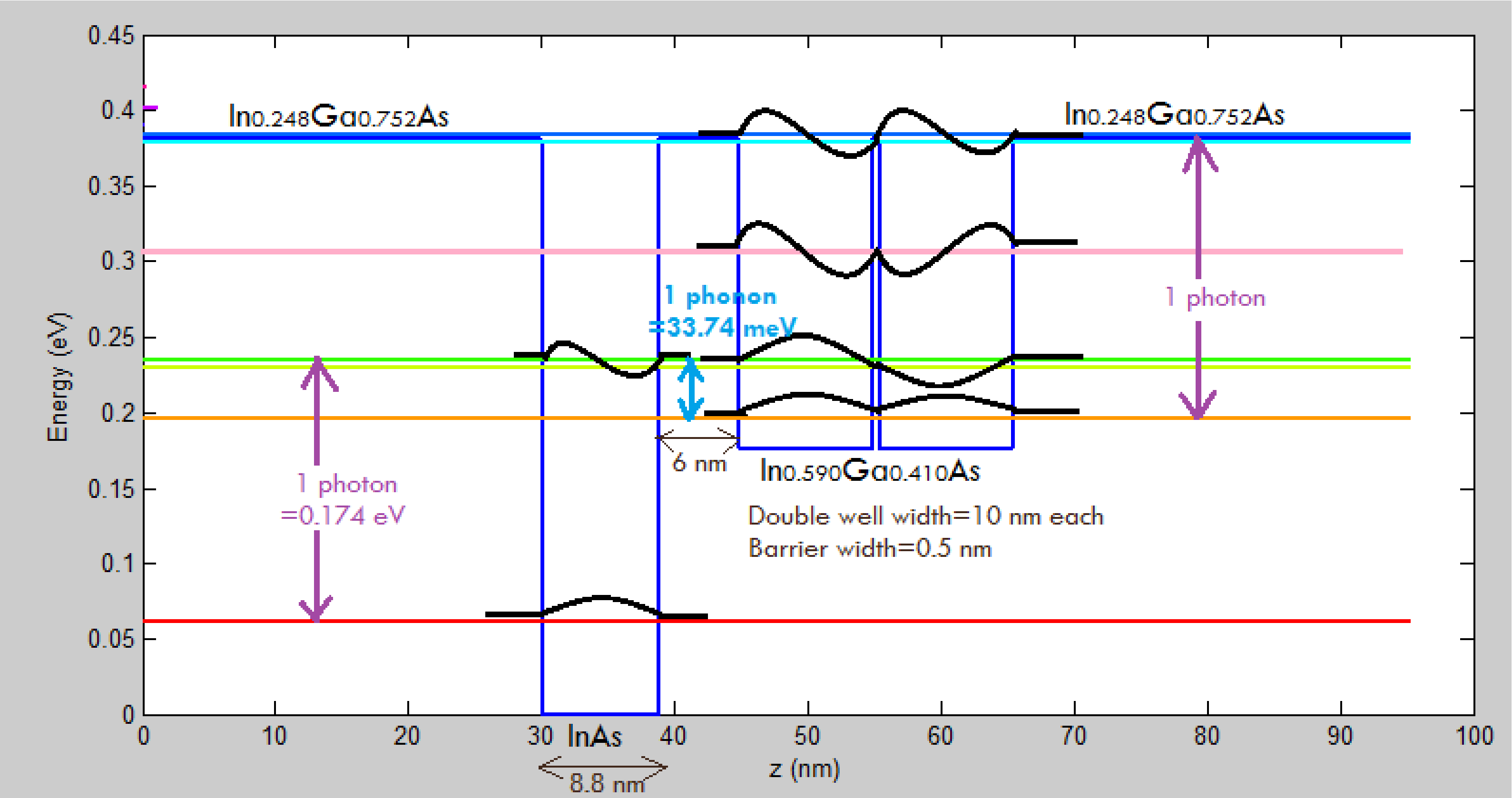

Energy (eV)
0.45
0.4
0.35
0.3
0.25
0.2
0.15
0.1
0.05
0
0
10
20
30
40
50
60
70
80
90
100
z (nm)
In0.248Ga0.752As
In0.248Ga0.752As
1 phonon
=33.74 meV
1 photon
1 photon
=0.174 eV
6 nm
In0.590Ga0.410As
Double well width=10 nm each
Barrier width=0.5 nm
InAs
8.8 nm

Let Us Meet Again

We welcome all to our future group conferences of Omics group international

Please visit:

www.omicsgroup.com

www.Conferenceseries.com

http://optics.conferenceseries.com/